# RADIOSYNTHESIS OF NOVEL 68Ga-LABELLED-α-CYCLODEXTRIN FOR PET IMAGING

Mr. Sirapop Sriaumpai

A Thesis Submitted in Partial Fulfillment of the Requirements
for the Degree of Master of Science in Pharmaceutical Sciences and
Technology
Faculty Of Pharmaceutical Sciences
Chulalongkorn University
Academic Year 2023

การสังเคราะห์สารรังสีแอลฟาไซโคลเด็กซ์ทรินติดฉลากแกลเลียม-68ชนิดใหม่สำหรับการ
ถ่ายภาพทางรังสีด้วยเครื่องเพ็ท

นายสิรภพ ศรีอำไพ

จุฬาลงกรณ์มหาวิทยาลัย
CHULALONGKORN UNIVERSITY

| | |
|---|---|
| Thesis Title | RADIOSYNTHESIS OF NOVEL 68Ga-LABELLED-α-CYCLODEXTRIN FOR PET IMAGING |
| By | Mr. Sirapop Sriaumpai |
| Field of Study | Pharmaceutical Sciences and Technology |
| Thesis Advisor | Associate Professor PHATSAWEE JANSOOK, Ph.D. |
| Thesis Co Advisor | Associate Professor SHUICHI SHIRATORI, Ph.D. |

Accepted by the FACULTY OF PHARMACEUTICAL SCIENCES, Chulalongkorn University in Partial Fulfillment of the Requirement for the Master of Science

............................................ Dean of the FACULTY OF PHARMACEUTICAL SCIENCES
(Professor PORNANONG ARAMWIT, Ph.D.)

THESIS COMMITTEE

............................................ Chairman
(Assistant Professor NARUEPORN SUTANTHAVIBUL, Ph.D.)

............................................ Thesis Advisor
(Associate Professor PHATSAWEE JANSOOK, Ph.D.)

............................................ Thesis Co-Advisor
(Associate Professor SHUICHI SHIRATORI, Ph.D.)

............................................ Examiner
(PATANACHAI LIMPIKIRATI, Ph.D.)

............................................ Examiner
(Assistant Professor KITIWAT KHAMWAN, Ph.D.)

............................................ External Examiner
(Associate Professor WARISADA SILAON, Ph.D.)

สิรภพ ศรีอำไพ : การสังเคราะห์สารรังสีแอลฟาไซโคลเด็กซ์ทรินติดฉลากแกลเลียม-68ชนิดใหม่สำหรับการ
ถ่ายภาพทางรังสีด้วยเครื่องเพ็ท. ( RADIOSYNTHESIS OF NOVEL 68Ga-
LABELLED-α-CYCLODEXTRIN FOR PET IMAGING) อ.ที่ปรึกษาหลัก : รศ.
ภก. ดร.ภาสวีร์ จันทร์สุก, อ.ที่ปรึกษาร่วม : รศ. ภก. ดร.ชูอิจิ ชิระโทริ

ไซโคลเด็กซ์ทริน คือโอลิโกแซ็กคาไรด์ที่เชื่อมต่อกันเป็นวงกลมประกอบด้วยหน่วยของกลูโคสที่เชื่อมกันด้วย
พันธะ $\alpha$-1,4 ไกลโคซิดิก โดยทั่วไปไซโคลเด็กซ์ทรินนำมาใช้เป็นสารช่วยทางเภสัชกรรม และมีประโยชน์หลากหลายใน
อุตสาหกรรมต่างๆ ปัจจุบันมีความสนใจประยุกต์ใช้ไซโคลเด็กซ์ทรินในการภาพถ่ายทางการแพทย์โดยเฉพาะในการภาพถ่าย
ทางเวชศาสตร์นิวเคลียร์ ในงานวิจัยนี้มีวัตถุประสงค์ในการสังเคราะห์สารรังสี $^{68}$Ga-alpha-cyclodextrin ($^{68}$Ga-
$\alpha$CD) โดยการติดฉลากสารรังสีแกลเลียม 68 กับ แอลฟาไซโคลเด็กซ์ทรินโดยตรง สารรังสีแกลเลียม 68 ถูกชะ ผสมกับ
สารละลายแอลฟาไซโคลเด็กซ์ทริน และทำปฏิกิริยาที่อุณหภูมิ 100 องศา เป็นเวลา 20 นาที หลังจากนั้นทำให้เย็นลงที่
อุณหภูมิห้อง วิเคราะห์ $^{68}$Ga-$\alpha$CD ที่เตรียมได้โดยแมสสเปกโตรเมตรี และการจำลองการจับกันด้วยคอมพิวเตอร์จากนั้นทำ
การคำนวณค่าความบริสุทธิ์ทางรังสี โดยใช้กระดาษโครมาโทกราฟี วัดค่าความเป็นกรดด่าง ปรับกระบวนการสังเคราะห์ติด
ฉลากให้เหมาะสมและทำให้บริสุทธิ์ขึ้น เพื่อเพิ่มค่าความบริสุทธิ์ทางรังสีของ $^{68}$Ga-$\alpha$CD โดยใช้สารเพิ่มความคงตัวทาง
รังสี ได้แก่ โซเดียมแอสคอร์เบต หรือกรดแอสคอร์บิก ใช้ความเข้มข้นของสารละลายแอลฟาไซโคลเด็กซ์ทรินต่างๆ (0.25–
5 มิลลิกรัมต่อมิลลิลิตร) การใช้แอลฟาไซโคลเด็กซ์ทรินพอลิเมอร์ และการทำให้บริสุทธิ์ด้วยตัวกรอง C-18 ในตอนเริ่มต้น
ค่าความบริสุทธิ์ทางรังสีของ $^{68}$Ga-$\alpha$CD นั้นต่ำมาก (0.24 ± 0.03%) แต่หลังจากปรับกระบวนการสังเคราะห์ติด
ฉลากให้เหมาะสมพบว่า การใช้โซเดียมแอสคอร์เบตร่วมกับความเข้มข้นของแอลฟาไซโคลเด็กซ์ทรินที่ 1 มิลลิกรัมต่อมิลลิลิตร
และการทำให้บริสุทธิ์ด้วยตัวกรอง C-18 ส่งผลให้ค่าความบริสุทธิ์ทางรังสีเพิ่มขึ้นอย่างมีนัยสำคัญ โดยค่าความบริสุทธิ์ทาง
รังสีที่ได้เท่ากับ 18.4 ± 1.1% ต่อมาได้มีการศึกษาไมโคนาโซล หรือไซโคลสปอริน เอ จับกับแอลฟาไซโคลเด็กซ์ทริน
ก่อนทำการติดฉลากกับสารรังสีแกลเลียม 68 ผลที่ได้พบว่าการใส่ยานั้น ไม่ส่งผลต่อการสร้างพันธะระหว่างสารรังสีแกลเลียม
68 และแอลฟาไซโคลเด็กซ์ทริน ซึ่งแสดงให้เห็นและยืนยันผลจากแมสสเปกโตรเมตรี และแบบจำลองการจับกันด้วย
คอมพิวเตอร์ พบว่าการจับกันของสารรังสีแกลเลียม 68 กับแอลฟาไซโคลเด็กซ์ทริน มีอัตราส่วนปริมาณสารสัมพันธ์เป็น 1:1
และตำแหน่งที่จับของสารรังสีแกลเลียม 68 อยู่บนขอบของส่วนปฐมภูมิ หรือทุติยภูมิในโครงสร้างของแอลฟาไซโคลเด็กซ์
ทริน

จุฬาลงกรณ์มหาวิทยาลัย
CHULALONGKORN UNIVERSITY

| | | |
|---|---|---|
| สาขาวิชา | เภสัชศาสตร์และเทคโนโลยี | ลายมือชื่อนิสิต ................................................. |
| ปีการศึกษา | 2566 | ลายมือชื่อ อ.ที่ปรึกษาหลัก ............................... |
| | | ลายมือชื่อ อ.ที่ปรึกษาร่วม ............................... |

# # 6470044933 : MAJOR PHARMACEUTICAL SCIENCES AND TECHNOLOGY

KEYWORD:   Cyclodextrin Radiopharmaceuticals Gallium-68 Radiochemical purity

Sirapop Sriaumpai : RADIOSYNTHESIS OF NOVEL 68Ga-LABELLED-α-CYCLODEXTRIN FOR PET IMAGING. Advisor: Assoc. Prof. PHATSAWEE JANSOOK, Ph.D. Co-advisor: Assoc. Prof. SHUICHI SHIRATORI, Ph.D.

Cyclodextrins (CDs) are cyclic oligosaccharides composed of glucose units linked by α-1,4 glycosidic bond. CDs are commonly used as pharmaceutical excipients and they offer versatile benefits in various industries. Recently, CDs have been promising for the application of medical imaging, especially nuclear medicine imaging. Herein, we aim to radiosynthesize $^{68}$Ga-alpha-cyclodextrin ($^{68}$Ga-αCD) by directly radiolabeling Ga-68 to αCD. Briefly, Ga-68 was eluted, mixed with αCD solution and heated at 100 °C for 20 min. Subsequently, the reaction was allowed to cool down at room temperature. The resulting $^{68}$Ga-αCD was characterized using mass spectrometry (MS) and elucidated by in silico computational studies. Radioactivity was measured using instant thin layer chromatography. The radiochemical purity (RCP) was calculated. The pH of the resulting solution was measured using a pH meter. The radiosynthesis process was then optimized and purified to increase the RCP of $^{68}$Ga-αCD. The radiostabilizers, i.e., sodium ascorbate or ascorbic acid, were selected, various concentrations of αCD solutions (0.25–5 mg/ml) and αCD polymer were included to optimize the process and C-18 cartridge was employed to purify $^{68}$Ga-αCD solution. Initially, the RCP of $^{68}$Ga-αCD is very low (0.24 ± 0.03%). Upon the optimization using sodium ascorbate as radiostabilizer together with 1 mg/ml αCD solution and further purification using C-18 cartridge, the RCP is significantly increased. Ultimately, we have successfully achieved an RCP of 18.4 ± 1.1%. Subsequently, miconazole or cyclosporin A was introduced into the αCD cavity prior to radiolabeling, but no significant impact on the binding affinity between Ga-68 and αCD was observed. This is subsequently confirmed by MS and computational studies that the stoichiometry ratio of Ga-68 and αCD is 1:1 complex and binding site of Ga-68 is on either primary or secondary rim of αCD.

| Field of Study: | Pharmaceutical Sciences and Technology | Student's Signature ............................... |
| Academic Year: | 2023 | Advisor's Signature ............................. |
| | | Co-advisor's Signature ......................... |

# ACKNOWLEDGEMENTS

# TABLE OF CONTENTS

**Page**

# LIST OF TABLES

จุฬาลงกรณ์มหาวิทยาลัย

CHULALONGKORN UNIVERSITY

# LIST OF FIGURES

# Chapter I
# Introduction

Cyclodextrins (CDs) are cyclic oligosaccharides consisting of glucopyranose units linked by α-1,4 glycosidic bonds. They possess cone-shaped structures capable of forming inclusion complexes, resulting in enhanced aqueous solubility of poorly water-soluble drugs. The natural CDs are α-cyclodextrin (αCD), β-cyclodextrin (βCD) and γ-cyclodextrin (γCD), which are composed of 6, 7, or 8 glucose units, respectively (1). The natural CDs and their guest/CD complexes have limited aqueous solubility. Various CD derivatives, such as hydroxypropyl and randomly methylated CDs, have been introduced to improve their solubility and that of their complexes (2). CDs are enabled excipients in pharmaceutical products, and they offer versatile benefits in many industries, such as food, textiles and packaging, cosmetics and personal care, and the separation process. Recently, CDs have been interesting for the application of medical imaging, especially in the field of nuclear medicine (3).

Nuclear medicine is a specialty within radiology, employs radiopharmaceuticals for diagnostic, therapeutic or theranostic purposes. While the primary route of administration for radiopharmaceuticals is intravenous, alternative routes such as ingestion or inhalation can be employed for specific agents (4). In the diagnostic approach, nuclear medicine employs advance imaging modality such as single photon emission computed tomography (SPECT) and positron emission tomography (PET) to detect the distribution and accumulation of radiopharmaceuticals within organ or tissue of patient's body (5). In the therapeutic approach, nuclear medicine utilizes high linear energy transfer (LET) radiopharmaceuticals to inflict damage on targeted cells or tissue. Its principle lies in cancer treatment, encompassing both curative and palliative treatment (6, 7). Moreover, it exhibits efficacy in treating micro-metastasis that cannot be detected by conventional imaging technique (8). In theranostic approach, it is considered as precision medicine. This approach is a combination of diagnostic and therapeutic approaches. It employs two radiopharmaceuticals sharing the same ligand but featuring different radionuclide. It is primarily used in oncology applications. Low

LET radionuclides such as Gallium-68 (Ga-68) are employed for pinpointing tumor site, meanwhile high LET radionuclides, for example, Lutetium-177 (Lu-177) are harnessed for neutralizing the tumor (8, 9).

Among all PET radionuclides, Ga-68 stands out as one of the most frequently employed radionuclides because it can be easily obtained from $^{68}$Ge/$^{68}$Ga generator (10). Its primary utilization lies in theranostic approach, often in conjunction with Lu-177 as previously mentioned above. However, the scope of its application extends beyond clinical use. Researchers have found its potential to be used in tracking specific molecules of interest by radiolabeling with Ga-68, enabling the observation of their biodistribution.

Hajdu et al. (2019) (11) studied the *in vivo* distribution of 2-hydroxypropyl-β-cyclodextrin (HPβCD) in normal mice by radiolabeling with $^{68}$Ga-1,4,7-triazacyclononane,1-glutaric acid-4,7-acetic acid (NODAGA). $^{68}$Ga-NODAGA-HPβCD has high radiochemical purity, stability, favorable pharmacokinetics in a mouse model and partition coefficient (log P value) at -3.07. One year later, the same research group investigated the biodistribution of the prostaglandin E2 (PGE2)/randomly methylated β-cyclodextrin (RMβCD) complex in normal mice and PGE2 positive tumor-bearing mice by radiolabeling with $^{68}$Ga-NODAGA (12). The log P value of $^{68}$Ga-NODAGA-RMβCD is -3.63. A high standard uptake value (SUV) and accumulation of $^{68}$Ga-NODAGA-RMβCD at the tumor site were observed in the tumor-bearing mice group. In mid-2022, Csige et al. (2022) (13) investigated the *in vivo* distribution of RMβCD in normal mice and tumor-bearing mice by radiolabeling with $^{68}$Ga- 1,4,7,10-tetraazacyclododececane,1-(glutaric acid)-4,7,10-triacetic acid (DOTAGA), and $^{205/206}$Bi-DOTAGA. The log P value of $^{68}$Ga-DOTAGA-RMβCD and $^{205/206}$Bi-DOTAGA are -3.47 and -3.45 respectively. Again, in the tumor-bearing mice, high SUV and accumulation of $^{68}$Ga-DOTAGA-RMβCD at the tumor site were also detected. In late 2022, Szabo et al. (2022) (14) evaluated the *in vivo* PET imaging of $^{68}$Ga-NODAGA- RMβCD and $^{68}$Ga-NODAGA-HPβCD compared with $^{18}$F-Fluorodeoxyglucose ($^{18}$F-FDG) in a tumor model. $^{68}$Ga-NODAGA-RMβCD and $^{68}$Ga-NODAGA-HPβCD uptake at the tumor site. However, the accumulation and SUV of both radiopharmaceuticals were lower than those of $^{18}$F-FDG.

As aforementioned above, CD-based radiopharmaceuticals have the potential for PET imaging and can be further developed and expanded for other applications in nuclear medicine. For example, tracking the biodistribution of drugs in a formulation containing CD as an excipient, the synergistic or additive effects of chemotherapy drug/CD complexes, and radiolabeled with β- or α-emitting radionuclide for tumor killing. Based on our best knowledge, there are no reports regarding direct radiolabeling between CDs and radionuclides. Thus, in this study, we performed and optimized a radiosynthesis of αCD labeled with Ga-68 ($^{68}$Ga-αCD) by directly labelling. αCD was selected due to its high aqueous solubility and applicable use in parenteral preparations. $^{68}$Ga-αCD was characterized in terms of the radiochemical purity (RCP) using thin layer chromatography (TLC). Mass spectrometry (MS), and the pH of solutions were also measured. The *in silico* computational study was carried out to identify the binding site of Ga-68 on αCD. Subsequently, the effect of radiostabilizers, the concentrations of ligand (i.e., αCD) were determined and the purification step using C-18 cartridge was performed for the optimization process. Finally, the effect of the drug binding capacity to αCD, the model drugs (i.e., miconazole and cyclosporin A) were incorporated in $^{68}$Ga-αCD solutions and the resulting RCP in the presence and absence drugs was compared. Therefore, the main objectives of this study are as follow:

- To develop and optimize a novel αCD directly labeled with Ga-68.
- To determine the drug binding capacity of neat αCD and $^{68}$Ga-αCD.

# Chapter II

# Literature review

## 2.1 Cyclodextrins

CDs are macrocyclic glucopyranose units composed of glucose units connected by α-1,4 glycosidic bond (1-3, 15, 16). CDs are produced from starch by the enzyme CD glucosyltransferase (CGTase). CDs are commonly used as pharmaceutical excipients due to their ability to form an inclusion complex with various guest molecules, mainly via van der Waals force. CDs are doughnut-shaped molecules with hydrophilic exterior and a somewhat lipophilic central cavity. In aqueous solutions CDs are able to form water-soluble inclusion complexes of lipophilic poorly soluble drugs by encapsulating some lipophilic moiety of the drugs into the central cavity (1) (Figure 1). The natural CDs, αCD, βCD and γCD correspond to 6, 7, and 8 glucopyranose units, respectively (Figure 2). All 3 natural forms are considered as safe by FDA (15). The CGTases are produced by a variety of bacteria, mainly Bacillus species (3, 16). Among the natural CDs, βCD has the lowest aqueous solubility due to its rigid structure. Meanwhile, the longer chain more flexible structure of γCD exhibits the highest aqueous solubility (16).
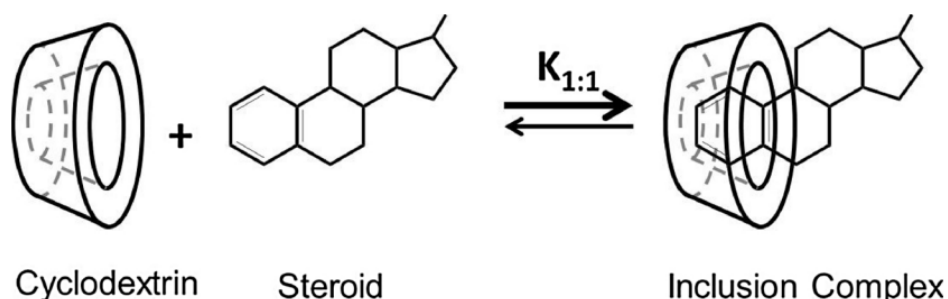


**Figure 1**. Formation of an inclusion complex in aqueous solution.
$K_{1:1}$ is the equilibrium constant (i.e. the stability constant) where 1:1 indicates the stoichiometry of the complex (1).
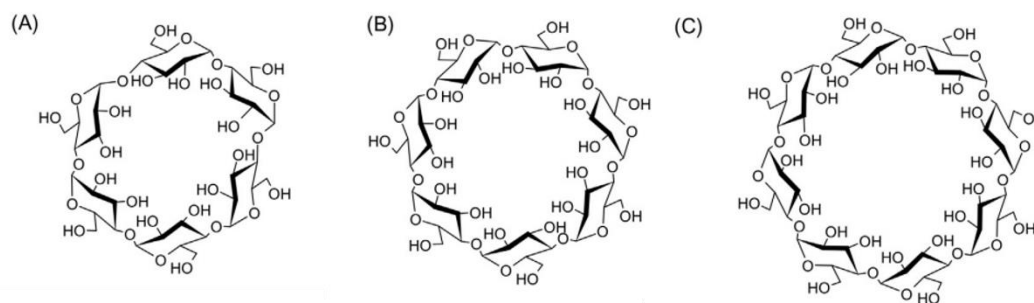
**Figure 2.** The structures of (A) αCD, (B) βCD, and (C) γCD. Adapt from (17)

To improve the solubility of natural CDs, the structure of natural CDs must be modified. Substitution of existing hydroxy group with hydroxypropyl, methyl or sulfobuthylether proves to be an effective way to improve not just solubility but also physiochemical and biological properties (2). There are three hydroxy groups on CD that can be modified. The first one is a hydroxy group at position 6 on the primary face or narrow rim of the molecule; it is the most basic and nucleophilic (Figure 3). The second hydroxy group is a hydroxy group in 2-position located on the secondary face or wide rim of the molecule; it is the most acidic group. The final hydroxy group is at 3-position, which is also located on the secondary face; it is the most inaccessible group (16, 18, 19). Table 1 shows the physiochemical properties of natural CDs and their derivatives.
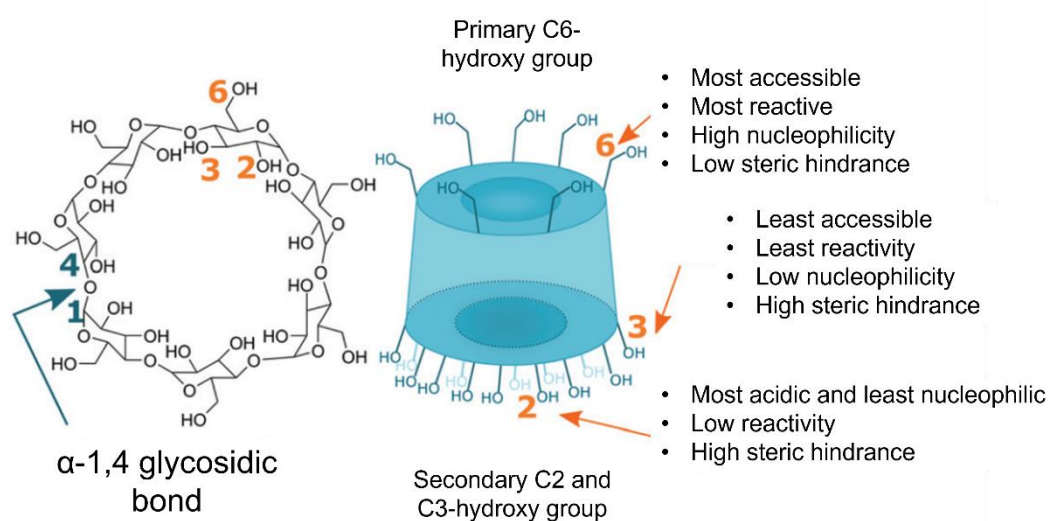


**Figure 3.** 3D structure of cyclodextrins. Adapt from (19)

**Table 1.** physiochemical properties of natural CDs and their derivatives (*Modified from* (16).

| Cyclodextrin | Number of substituents[a] | Molecular weight (g/mol) | Solubility in water (mg/ml)[b] |
|---|---|---|---|
| α-Cyclodextrin (αCD) | - | 972 | 145 |
| β-Cyclodextrin (βCD) | - | 1135 | 18.5 |
| γ-Cyclodextrin (γCD) | - | 1297 | 232 |
| 2-Hydroxypropyl-αCD (HPαCD) | 3.6 | 1199 | >500 |
| 2-Hydroxypropyl-βCD (HPβCD) | 2.8-10.5 | 1400 | >600 |
| Randomly methylated-βCD (RMβCD) | 9.7-13.6 | 1312 | >500 |
| Hydroxyethyl-βCD (HEβCD) | 3.6 | 1443 | >2000 |
| Sulfobutylether-βCD (SBEβCD) | 6.2-6.9 | 2163 | >500 |
| 2-Hydroxypropyl-γCD (HPγCD) | 3.0-5.4 | 1576 | >500 |

[a] The average number of substituents per one CD molecule. [b] The solubility in pure water at 25°C

## 2.2 Radiopharmaceuticals

Radiopharmaceuticals are biological radioactive compounds capable of acting as diagnostic and/or therapeutic agents, depending on the type of labeled radionuclides. γ and positron-emitting radionuclides such as Tc-99m and Ga-68 are used in the diagnosis role due to their low LET, whereas α- and β-emitting radionuclides such as Ac-225 and Y-90 are used in the therapeutic role due to their high LET which capable of inducing DNA strand break (20). However, there are

some radionuclides that are considered as theranostic agents, such as Iodine 131 (I-131), due to the emission of both β particles and γ-rays (20-22). Radiopharmaceuticals usually consist of four parts (Figure 4). The first one is a radionuclide, which emits radiation. The second is a chelator, which binds to radionuclides. The third is the linker, which links the chelator with the ligand; sometimes it can be modified to increase the biological half-life of the compound. The fourth is ligand, which is responsible for binding to the specific receptor on the target organ (21). Radiopharmaceuticals play an important role in several clinical uses like in oncology, cardiology, neurology, and nephrology. Radiopharmaceuticals are also very useful in preclinical study as well. It allows researchers to monitor the cells which are helpful in cell therapy like cancer immunotherapy (23). To detect radiopharmaceuticals, an imaging instrument is needed. Nowadays, the most commonly used instruments are SPECT and PET scans (20-22, 24).
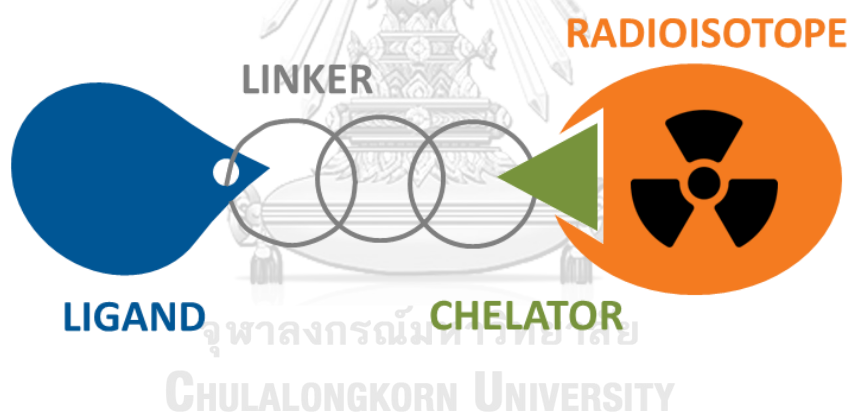


**Figure 4.** Radiopharmaceutical's structure

Figure credit: Admare bioinnovation. Radiopharmaceuticals: a new class of drugs for cancer patients and a new road for Canada to lead global life sciences [Internet]. 2020 [cited 2023 May 29]. Available from: https://www.admarebio.com/en/news-details/radiopharmaceuticals-a-new-class-of-drugs-for-cancer-patients-and-a-new-road-for-canada-to-lead-global-life-sciences

2.2.1 Use of radiopharmaceuticals in clinic

In oncology, there are varieties of radiopharmaceuticals that can be employed. $^{18}$F-FDG is commonly employed to detect early-stage and recurrence cancer. It is a glucose analogue which will be highly uptake and accumulate in tumor cells (25). $^{99m}$Tc-methyl diphosphonate (MDP) can detect bone metastasis due to it typically uptake in area that has high bone turnover or bone formation (26). $^{177}$Lu- prostate-specific membrane antigen (PSMA) emits β- particle that can neutralize prostate cancer cells (22). I-131 is a radioisotope of iodine which is normally uptake by thyroid glands. It emits both γ-ray and β particle, which allowing it to be used for both diagnose and treat thyroid cancer (27). In cardiology, $^{99m}$Tc-red blood cell (RBC) is used in multigated acquisition (MUGA) scan for evaluate left ventricle ejection fraction. $^{99m}$Tc-setamibi, $^{13}$N-ammonia, $^{15}$O-water or $^{82}$Rb can be used for myocardial perfusion scan to evaluate coronary artery stenosis (24, 27). In neurology, $^{99m}$Tc-ethyl cysteinate dimer (ECD) and $^{99m}$Tc-hexamethylpropyleneamine oxime (HMPAO) are used for brain perfusion scan to evaluate dementia or epilepsy (28, 29). $^{18}$F-fluoro-l-dopa (FDOPA) is used for brain tumor imaging. $^{18}$F-FDG is used for Alzheimer disease diagnosis (24, 27). In nephrology, $^{99m}$Tc- mercaptoacetyltriglycine (MAG3), $^{99m}$Tc- diethylene triamine pentaacetic acid (DTPA) and $^{99m}$Tc- dimercaptosuccinic acid (DMSA) can be used for renal scan (30).

2.2.2 Use of radiopharmaceuticals in preclinical research

In preclinical research, radiopharmaceuticals can be used for either *in vivo* molecular tracking or cellular tracking. For molecular tracking, the molecule of interested can be labeled with radionuclide, enabling the determination of molecule distribution (31). For example, Cu-64 has been radiolabeled with DOTA and subsequently bound to camptothecin conjugated with a βCD polymer. This approach enables the tracking of the drug's biodistribution and the acquisition of pharmacokinetic data (3). In case of cellular tracking, stem cells or some immune cells like cytotoxic T cells and dendritic cells can be radiolabeled with radioisotope

either by direct or indirect technique (23). Direct cell labeling method is the most used method due to its simple, safety, and easy to translate into clinical use. The radiopharmaceutical will either bind directly to cell membrane or enter the cell via passive diffusion, uptake by transporter protein, endocytosis, or phagocytosis. However, this method has some minor drawbacks (23, 32). First, the concentration of radiopharmaceuticals will be diluted if the target cells undergo cell division. Secondly, sometimes labeled radiopharmaceuticals can be released from target cells. Therefore, hindering the effectiveness in long-term imaging of the cells (23, 32, 33). Indirect cell labeling methods have been introduced to overcome those problems. Although the mechanism is quite similar, it is more complicated and costly than direct cell labeling method. Target cells need to have an express of reported gene. Therefore, target cells need to be genetically modified before labeling with radiopharmaceuticals (23, 32).

2.2.3 Quality control of radiopharmaceuticals

Prior to patient administration, quality control procedures have to be performed to ensure optimum characteristic of synthesized radiopharmaceutical. Appearance is one of quality parameters, which is primarily verified by visual observations. pH measurement is normally performed using a pH strip (10). Some metals like Fe, Ni, Cu, Zn and Pb are used as components inside the column of the generator. These metals are impurity when they are co-eluted with a desired radioisotope out from the generator. They are normally determined by inductively coupled plasma-mass spectrometry (ICP-MS) (34). Radionuclidic purity, which is an amount of desired radionuclide in total radiopharmaceutical, is determined by using gamma spectroscopy (35). Radiochemical purity (RCP) is the amount of desired radiopharmaceutical in total radiopharmaceuticals. It is measured using radio HPLC, that has radioactivity detector, or TLC (36). In the case of TLC, the radioactivity TLC paper is measured by $\gamma$ counter (Figure 5). The $\gamma$ counter detects $\gamma$ ray that interacts with its crystal. The interacting crystal emits light which is detected by the detector. The detected light was then amplified by photomultiplier. Finally, the light are

convert into electronic signal and then display on monitor screen (37). However, many of the tests cannot be performed before the administration due to limitation in physical half-life. Some of the tests like sterility and bacterial endotoxin test required considerable amount of time to complete (35). Therefore, radiopharmaceuticals are normally given to patients without waiting for sterility and bacterial endotoxin test results. To ensure safety, before administration of any radiopharmaceuticals to patient, it must be filtered by sterile filter. However, sterility tests using fluid thioglycolate medium and soybean-casein digest medium, and bacterial endotoxin test using limulus amebocyte lysate test still needed to be done in order to keep record (38, 39).
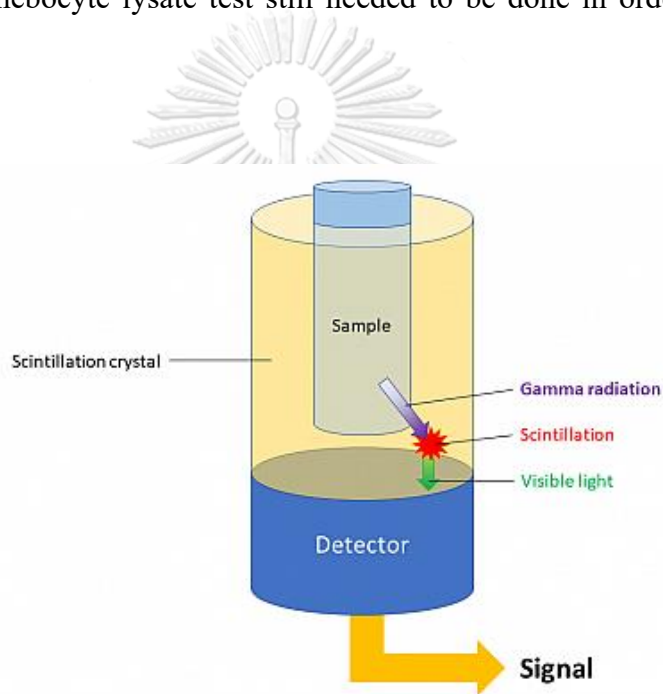


**Figure 5.** γ counter principle

Figure credit: Berthold Technologies. Gamma counter [Internet]. 2023 [cited 2023 November 23]. Available from:

https://www.berthold.com/es/bioanalytic/products/gamma-counters/

**2.3 Production and application of Gallium-68**

Ga-68 is a positron-emitting radioisotope of gallium. Ga-68 mainly emits positrons (89%), with the highest energy at 1.9 MeV and the average energy at 0.91 MeV (40). Ga-68 decays to Zn-68 with a relatively short physical half-life of 68 minutes (Figure 6), which is suitable for clinical use (41, 42). Generally, the cost of production is relatively low due to the fact that Ga-68 does not necessarily require a cyclotron. It can be obtained from the $^{68}$Ge/$^{68}$Ga generator (Figure 7) using hydrochloric acid (HCl). Once Ga-68 is obtained in the form of $^{68}$GaCl$_3$, it will be in a trivalent form (Ga 3+), which is capable of forming a stable complex with a chelator, such as DOTA through the chelation method. Ga-68 plays an important role in theranostic application because chelators like DOTA can also form complexes with Lu-177 and Ac-225 for therapeutic purposes (40-42). Ga-68 has shown many clinical uses, especially in oncology, such as for prostate cancer imaging using $^{68}$Ga-PSMA (Figure 8) which is a transmembrane glycoprotein enzyme that over-expresses on prostate cancer (43). Ga-68 can also be used in neuroendocrine tumor (NET) imaging which utilizes $^{68}$Ga-DOTA/NOTA-peptide like Tyr3-Octreotate (TATE)/Phe1-Try3-Octreotide (TOC)/NaI3-Octreotide (NOC) which are somatostatin analogs that bind to somatostatin receptors (SST) over-expressed on NET (44).

$$^{68}_{32}Ge + ^{0}_{-1}e \longrightarrow ^{68}_{31}Ga$$

$$^{68}_{31}Ga \longrightarrow ^{68}_{30}Zn + ^{0}_{+1}e$$
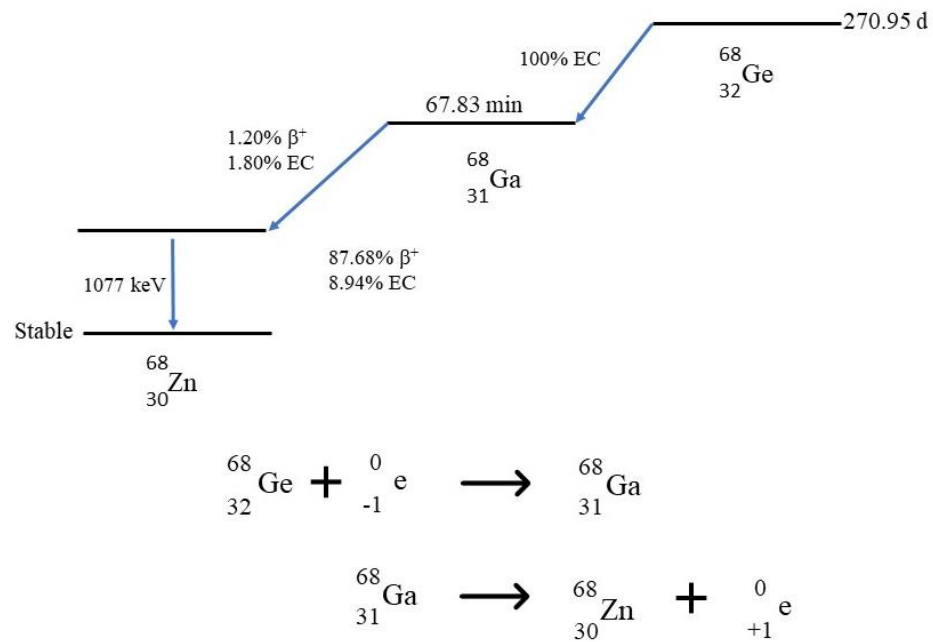
**Figure 6.** Ga-68 decay scheme. Adapt from (45)
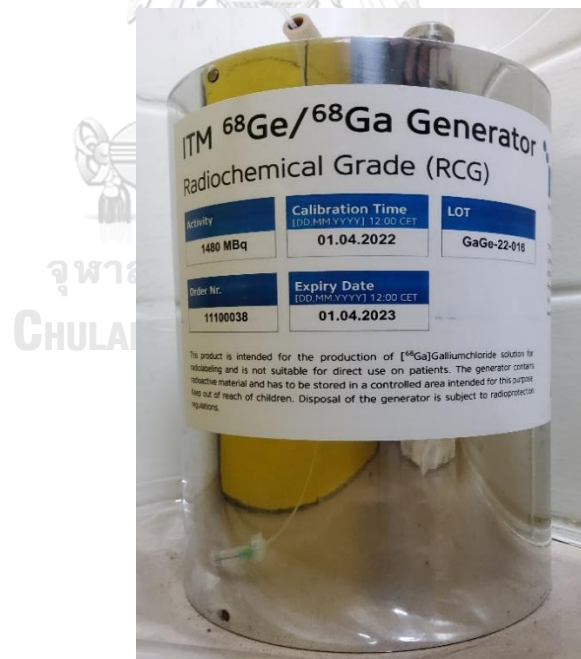


**Figure 7.** $^{68}Ge/^{68}Ga$ generator
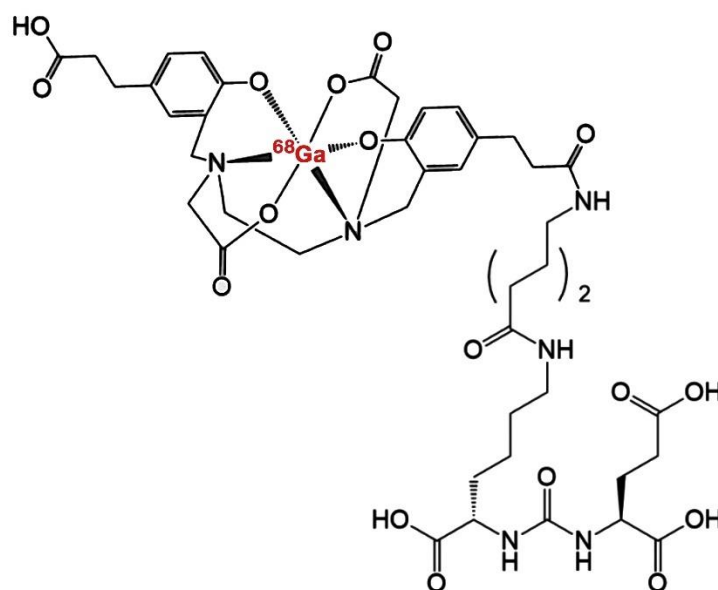
**Figure 8.** ^{68}Ga-PSMA-11

Figure credit: Wikipedia. Gallium 68 PSMA 11 [Internet]. 2021 [cited 2023 November 14]. Available from:

https://en.wikipedia.org/wiki/File:Gallium_68_PSMA-11.jpg

## 2.3.1 Production of Gallium-68 using [68]Ge/^{68}Ga generator

The easiest way to obtain Ga-68 is from the [68]Ge/^{68}Ga generator. The parent radioisotope is germanium-68 (Ge-68), which has a relatively long physical half-life of 271 days. The first [68]Ge/^{68}Ga generator was introduced around 1960 (46). To elute Ga-68, low concentration of ethylenediaminetetraacetic acid (EDTA) is required. The obtained Ga-68 is in form of ^{68}Ga-EDTA. Nowadays, the Ga-68 is eluted by using low concentration of HCl (46). HCl interacts with Ga-68 inside the generator resulting in the product in form of [68]GaCl$_3$. Consequently, the generator can continuously generate Ga-68 for a year (34, 41). However, the generator should be eluted every day or pre-elute 1 day before intended use in order to avoid Ge-68 breakthrough, which is a contaminant of Ge-68 in elution (34). Once Ga-68 is eluted from the generator, it is essential for the generator to undergo a waiting period until it nearly attains equilibrium before the elution process can be repeated. The equilibrium is the condition that daughter radioisotope concentration is equal to parent radioisotope concentration. In the specific case of Ge-68 and Ga-68 the equilibrium is called

secular equilibrium (Figure 9). The secular equilibrium is characterized by the parent radioisotope having a much longer physical half-life than daughter radioisotope (more than 100 times longer). This results in steady concentration of the parent radioisotope (47). Ga-68 has secular equilibrium at 14 h after the elution. However, it is not necessary to wait for 14 h in order to elute Ga-68 again. After 4 h post elution, the accumulation reaches over 90% and reach close to 100% after 6 h post elution. Therefore, if required the generator can be eluded every 4 h (34, 47).
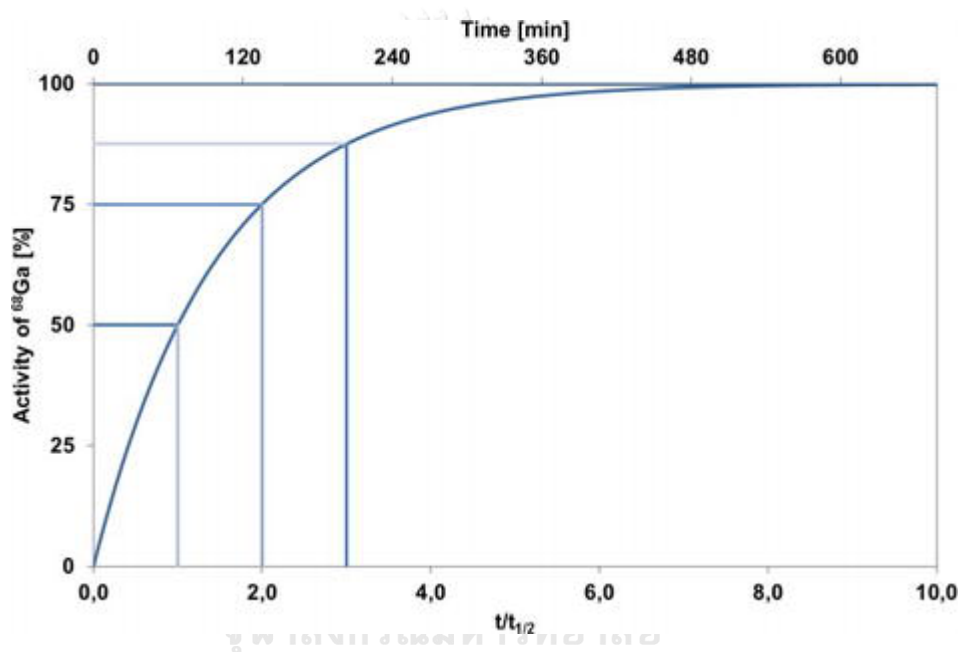


**Figure 9**. Secular equilibrium of Ga-68 (48)

2.3.2 Production of Gallium-68 using cyclotron

Ga-68 can still be obtained through the $^{68}Zn(p,n)^{68}Ga$ reaction using a cyclotron, with the option of employing either a solid or liquid target (10, 34). In case of liquid target, the target is Zn-68 solution typically in form of $^{68}Zn(NO_3)_2$ or $^{68}ZnCl_2$. Generally, $^{68}Zn(NO_3)_2$ is more preferred due to $^{68}ZnCl_2$ can cause radiolysis to the overall Zn 68 solution (10). The target is bombarded by 12–14 MeV beam energy. The cyclotron feature water and helium as a cooling system to combat heat generated from the bombardment. The yield of Ga-68 is mainly dependent on the Zn-68 concentration and the pressure during the bombardment (10). In the case of solid

target, the target is a Zn-68 powder compressed in a pellet. The target is then bombarded with the same energy beam for liquid target. In general, Zn-68 solid target yield higher $^{68}GaCl_3$ than the liquid counterpart due to its denser of Zn-68 in given area (10). The main disadvantage of using cyclotron in the production of Ga-68 is that the obtained product have to be purified to remove Zn-68 impurity, resulting in overall lower $^{68}GaCl_3$ yield (34). Increasing of beam energy can increase Ga-68 yield, but it also increases unwanted Ga-67 which is not suitable for PET imaging due to it emits γ ray (10).

## 2.4 Radiolysis and radiostabilizer

Radiolysis or radiolytic degradation, is the degradation of compounds that prevents product formation caused by free radicals. Free radicals are induced by ionizing radiation, such as α-, β- and γ-rays emitted from radionuclides (10, 49-51). A radiostabilizer, or radioprotectant, is a radical scavenger that can prevent the formation of free radicals (Figure 10). A good radiostabilizer should not interfere with the radiolabeling process, change the pH of solution, or interact with starting materials or radionuclides (49-51). There are some radiolabeling agents that are commonly used for radiolabeling processes, such as ascorbic acid, sodium ascorbate, acetate buffer, gentisic acid, etc. Due to each compound having different physical and chemical properties, selecting a suitable radiostabilizer is very important (10, 51). Therefore, it is worth considering which radiostabilizer is most suitable when developing new radiopharmaceuticals (10, 49-51).
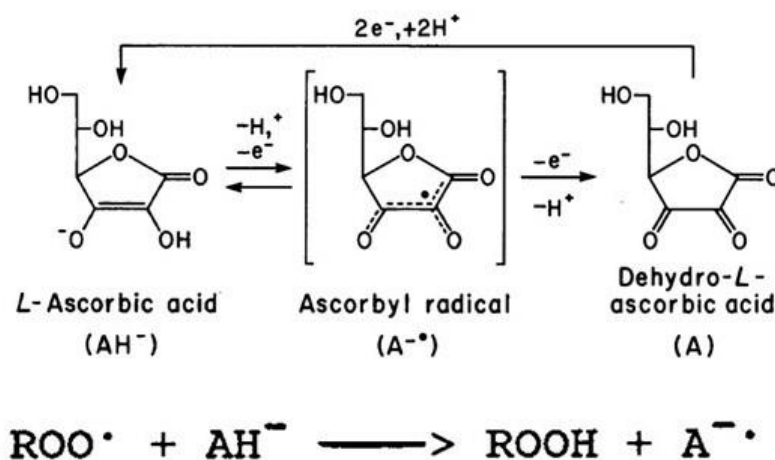
**Figure 10.** Mechanism of ascorbic acid as an antioxidation (52)

## 2.5 PET imaging

PET is a non-invasive imaging technique in nuclear medicine. Not all radioisotopes are suitable for PET scans; only positron-emitting radioisotopes have the capability (Table 2). PET scan machine detects two gamma rays produced by the annihilation reaction by using a ring detector (Figure 11). An annihilation reaction is a reaction in which electrons in the subject body interact with positrons emitted from a radioisotope. This interaction produces two gamma rays with a tilt angle of 180 degrees and energy at 511 keV (53). The two gamma rays are detected by ring detector inside the scanner within a limited time window usually around 4 – 12 ns (27, 53). There are three types of coincidences that can occur in PET: true, scattered, and random coincidences. Only true coincidence is relevant for image reconstruction. The reconstruction is carried out by an algorithm like iterative reconstruction method (53). PET imaging is a highly sensitive imaging technique that can provide a series of 3D images (53, 54). This technique is useful in scientific research for tracking down the in vivo biodistribution of molecules of interest labeled with radionuclides in real time and in clinical applications such as oncology, neurology, cardiology, and infectious disease (53-55). The main downside of PET is its low spatial resolution around 5-7

mm (27, 56). To overcome this problem, PET is usually paired with CT (Figure 12) which not only provides accurate anatomical position, but also provides attenuation value based on the attenuation coefficient of different tissues (27, 56). CT scan is a bore-shape instrument like PET scan. It consists of X-ray tube and detector with 180 degrees tilt angle. The tube and detector rotate simultaneously during image acquisition (56). CT usually generates photons with energy around 100 – 150 keV. Therefore, the obtained attenuation value needs to be scaled up to 511 keV for PET image attenuation correction (27, 56).
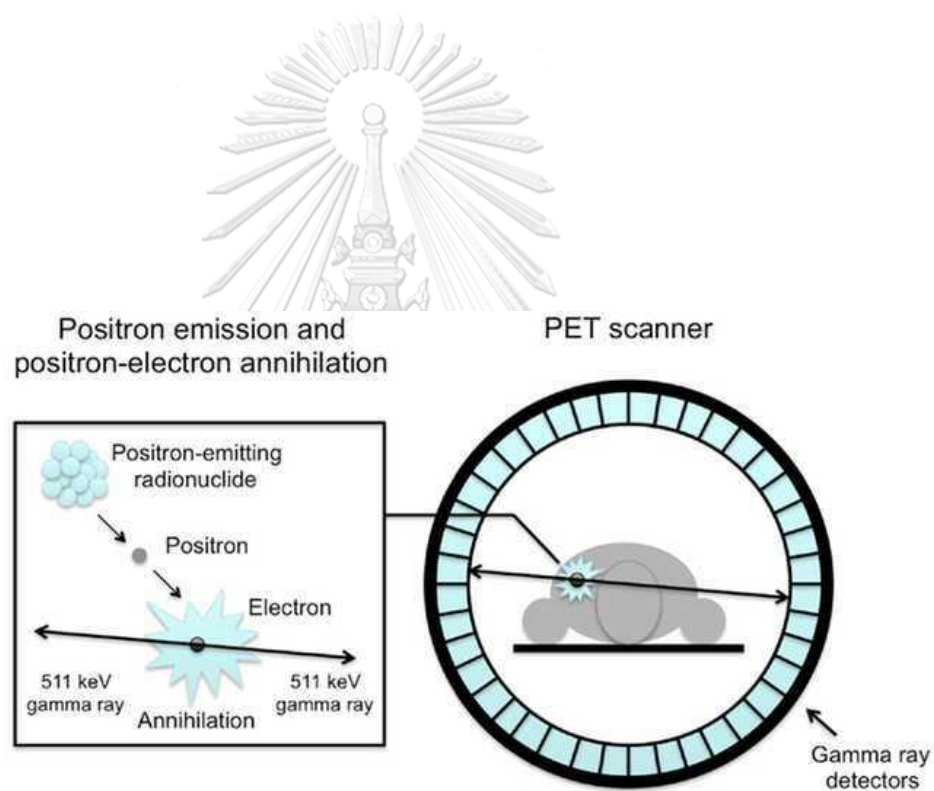


**Figure 11**. Principle of PET imaging

Figure credit: PhysicsForums. Learn the basics of positron emission tomography [Internet]. 2016 [cited 2023 May 1]. Available from:

https://www.physicsforums.com/insights/basics-positron-emission-tomography-pet/

**Figure  12**. PET/CT scanner

Figure credit: Siemens Healthineers. Biography vision [Internet]. 2018 [cited 2023 July 31]. Available from: https://www.siemens-healthineers.com/en-uk/molecular-imaging/pet-ct/biograph-vision

**Table 2.** Radioisotope used in PET scan *(modified from Ref (23, 27))*

| Radioisotope | Physical half life | Decay | Production method |
| --- | --- | --- | --- |
| Oxygen-15 | 2 min | Positron | Cyclotron |
| Nitrogen-13 | 10 min | Positron | Cyclotron |
| Carbon-11 | 20 min | Positron | Cyclotron |
| Gallium-68 | 68 min | Positron, electron capture | Generator |
| Fluorine-18 | 110 min | Positron, electron capture | Cyclotron |
| Cupper-64 | 12.7 h | Positron, electron capture | Cyclotron |
| Zircornium-89 | 78.4 h | Positron, electron capture | Cyclotron |
| Iodine-124 | 4.2 days | Positron, electron capture | Cyclotron |

จุฬาลงกรณ์มหาวิทยาลัย
CHULALONGKORN UNIVERSITY

# Chapter III
# Materials and Methods

## 3.1 Materials

αCD was kindly donated by Wacker Chemie (Munich, Germany). Soluble αCD polymer crosslinked with epichlorohydrin was purchased from Cyclolab R&D (Budapest, Hungary). Miconazole was purchased from Fagron group B.V., (Rotterdam, the Netherlands). Cyclosporin A was purchased from GenWay BioTech Inc. (San Diego, USA). Ga-68 solution was eluted from ITM $^{68}$Ge/$^{68}$Ga generator (radiochemical grade). 1,4,7,10-tetraazacyclododecane-1,4,7,10-tetraacetic acid (DOTA) was purchased from Chematech (Dijon, France). Sodium ascorbate was purchased from Tokyo Chemical Industry (Tokyo, Japan). Ascorbic acid was purchased from MySkinRecipes (Bangkok, Thailand). Sep-Pak C-18 cartridges were purchased from Waters (Massachusetts, USA). Other chemical reagents were provided by the Division of Nuclear Medicine, Department of Radiology, Faculty of Medicine, Siriraj Hospital, Mahidol University.

## 3.2 Methods

### 3.2.1 Radiosynthesis of $^{68}$Ga-DOTA and $^{68}$Ga-αCD

The radiosynthesis procedure is modified based on the clinical use of the PSMA-11 radiolabeling protocol (57). In this study, αCD was used as a ligand due to its high aqueous solubility and can be used in various pharmaceutical dosage forms, especially in parenteral solution (58). Briefly, 250 mg of αCD was accurately weighed, dissolved, and adjusted with sterile water to 100 mL (2.5 mg/ml). Further dilution was prepared by pipetting 1 ml of obtained αCD solution into a 10-ml volumetric flask and then adjusting the volume with sterile water to obtain the final concentration (0.25 mg/ml). After that, 100 µl of αCD solution was pipetted and mixed with 2 ml of 0.05 M HCl in a syringe. To compared with the reference, DOTA, the most commonly used as a chelator for Ga-68 (Figure 13) was prepared with the same procedure as described above (59).

For the Ga-68 eluting process, the reaction vial was put in shielding and connected to the $^{68}$Ge/$^{68}$Ga generator. Then, Ga-68 was eluted from the generator by using 4 ml of 0.05M HCL as an eluent. Radioactivity was measured immediately after

the elution. The obtained $^{68}$GaCl$_3$ solution was divided into two reaction vials. DOTA and αCD solutions that were previously prepared were separately added to the reaction vial. Both vials were heated at 100 °C for 20 minutes. After that, the reaction was allowed to cool down at room temperature for 5 minutes. Finally, the radioactivity was measured using instant thin layer chromatography (iTLC), and the presenting result data was RCP (Figure 14 and 15). Each sample was performed in triplicate.
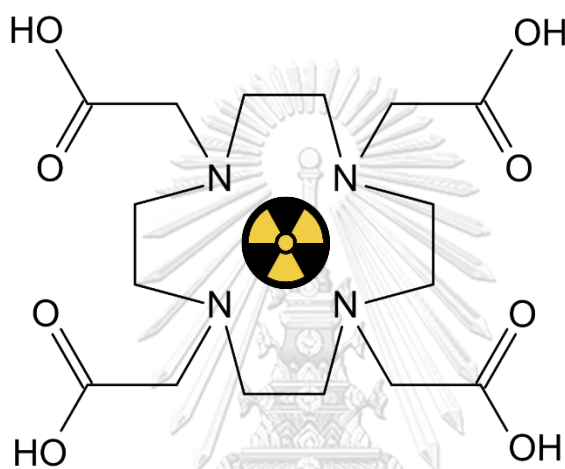


**Figure 13.** $^{68}$Ga-DOTA structure
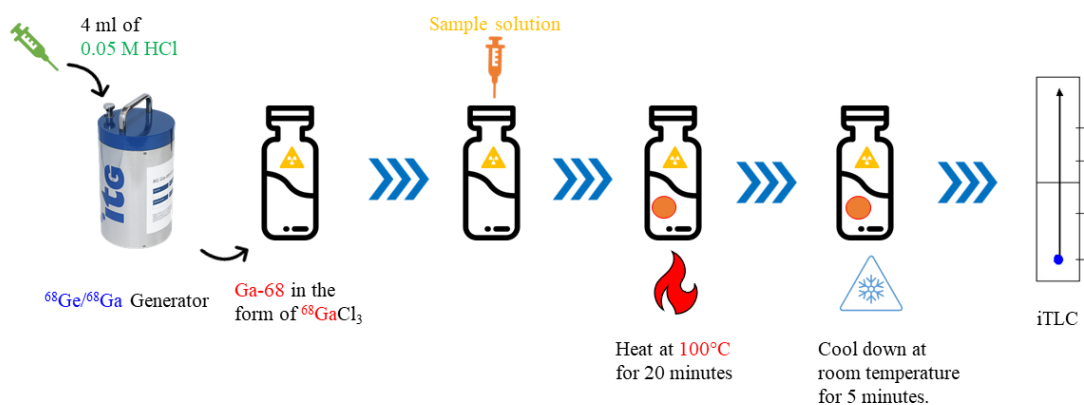


**Figure 14.** Radiosynthesis of $^{68}$Ga-DOTA and $^{68}$Ga-αCD

$$2[^{68}Ga]_{(s)} + 6HCl_{(aq)} \longrightarrow 2[^{68}GaCl_3]_{(aq)} + 3H_2{}_{(g)}$$

$$^{68}GaCl_3{}_{(aq)} + DOTA^{3-}{}_{(aq)} \xrightarrow[100°C,\ 20\ min]{\ } {}^{68}Ga\text{-}DOTA_{(aq)} + 3Cl^-{}_{(aq)}$$

$$^{68}GaCl_3{}_{(aq)} + \alpha CD^{3-}{}_{(aq)} \xrightarrow[100°C,\ 20\ min]{\ } {}^{68}Ga\text{-}\alpha CD_{(aq)} + 3Cl^-{}_{(aq)}$$
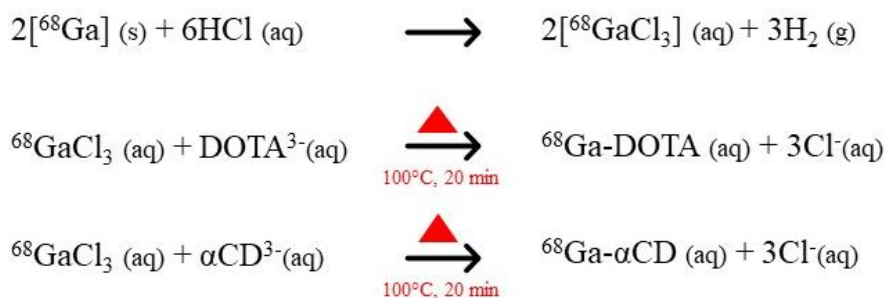
**Figure 15.** Chemical reaction during radiosynthesis of $^{68}$Ga-DOTA and $^{68}$Ga-αCD

### 3.2.2 Optimization of radiosynthesis

To optimize the radiosynthesis, the effect of radiostabilizers on the RCP of the $^{68}$Ga-DOTA and $^{68}$Ga-αCD, various αCD concentrations and the use of its derivative, soluble αCD polymer were determined on the RCP of $^{68}$Ga-αCD, and finally, the purification step using C-18 cartridge was performed.

### 3.2.2.1 Effect of radiostabilizer

Sodium ascorbate and ascorbic acid were selected as radiostabilizers. These two radiostabilizers have been reported as effective radiostabilizers for many radiopharmaceuticals (60). Each compound was separately prepared by dissolving 0.04 g in 2 ml of sterile water. Each solution was mixed with 100 µl of DOTA or αCD solutions and used as a ligand sample. The radiosynthesis process was conducted as described above. Each sample was performed in triplicate.

### 3.2.2.2 Effect of αCD concentration and αCD polymer

A stock solution of αCD was prepared by dissolving 500 mg of αCD in 100 ml of sterile water (5.0 mg/ml). Serial dilutions of αCD solutions were prepared, and the concentration range from 0.5 to 5.0 mg/ml were given. To assess the effect of three-dimensional polymer on degree of radiolabeling, 50 mg of soluble αCD polymer crosslinked with epichlorohydrin was accurately weighed, dissolved, and adjusted with sterile water to 50 ml (1 mg/ml).100 µl of resulting αCD solution or αCD polymer was mixed with 2 ml of sodium ascorbate solution (2% w/v). The

radiosynthesis process was conducted as described above. Each sample was performed in triplicate.

### 3.2.2.3 Purification of $^{68}$Ga-αCD

$^{68}$Ga-αCD was purified by C-18 cartridge. Firstly, the C-18 cartridge was washed with 2 ml ethanol prior to radiosynthesis process. After the radiosynthesis, waste vial was put in shielding and connected to the C-18 cartridge. $^{68}$Ga-αCD solution in reaction vial was drawn via syringe and connected to C-18 cartridge. The solution was pushed slowly through the C-18 cartridge. Subsequently, the C-18 cartridge was transferred to connect with product vial, which is in another shielding. C-18 cartridge was slowly flushed with 3 ml of 1:1 ethanol:water. Finally, the radioactivity and RCP of solution from product and waste vials were determined.

### 3.2.3 Chemical analysis

### 3.2.3.1 TLC and RCP determination

0.2 ml of sample ($^{68}$Ga-DOTA or $^{68}$Ga-αCD) were drawn in 1-ml syringe. Five small drops of the sample solution were dropped on iTLC paper. The paper was placed in a mobile phase tank containing 1 ml of 1:1 ammonium acetate:methanol. To determine TLC, the iTLC papers were scanned by TLC scanner (Gamma BGO-V-Detector, Raytest®, Isotopenmessgeraette, GmbH, Germany). For RCP measurement, the paper was cut into eight sections and put in eight separate tubes. After that, the activity of iTLC paper was measured in a well-chambered γ-counter. The RCP of the obtained product was calculated using the following equation:

$$RCP = (\text{Product} / [\text{Product} + \text{Free Ga-68}]) \times 100$$

### 3.2.3.2 Mass spectrometry

Qualitative analysis of $^{68}$Ga-αCD involved determining the mass-to-charge ratio (m/z) of $^{68}$Zn-αCD by MS after 3 days of radiolabeling. This time frame ensured the complete decay of all Ga-68 into Zn-68. The sample was analyzed by ESI (+) triple quadrupole MS (QTRAP6500, Sciex, Framingham, MA, USA) and DART (+) time of flight MS (AccuTOF™ LC-Express Time-of-Flight Mass Spectrometer, JEOL, USA). In the case of ESI (+) triple quadrupole MS, $^{68}$Ga-αCD was placed directly at ESI source and the analysis conditions were as follows: electrospray

ionization (ESI) positive mode; scan, 200–1050 m/z; temperature, 350 °C; capillary voltage, 4500 V; and collision energy, 40 eV.  In the case of DART (+) time of flight MS, ^{68}Ga-αCD was placed directly at DART source and the analysis conditions were as follows: DART positive mode; scan, 200–1050 m/z; helium gas temperature, 350 °C; detector voltage, 2000 V; ion guide RF voltage, 600 V; reflection voltage, 960 V; flight tube voltage' 7000 V and orifice voltage, 10-90 V. The expected mass-to-charge ratio is 1041.3 g/mol ^{68}Ga-αCD.

### 3.2.3.3 pH measurement

pH of the obtained sample was determined using a pH meter (FE20 FiveEasy, Mettler Toledo, Switzerland) at 25 °C. Prior to analysis, the pH meter was calibrated with the standard solutions at the pH of 4, 7 and 10.

### 3.2.4 In silico computational study using Quantum Mechanics

The initial structure of αCD was obtained from PDB (ID: 7uww), illustrated in Figure 16. The gallium ($Ga^{3+}$) cation was placed on both primary and secondary rim of αCD and four water molecules were added explicitly by using GaussView 6.0. The computations were performed using the Gaussian 09 software suite. Optimal geometries for all studied systems were obtained using density functional theory (DFT) by applying the UB3LYP level of theory (61) with a 6-31G (d, p) basis set. To conduct computations in aqueous environments, the Conductor-Like Polarizable Continuum Model (CPCM) is commonly employed as a water model. This PCM variant incorporates the charge-transfer effect as an integral aspect of solvation (62). Adsorption energy, an energy required for a molecule or a system to absorb a photon and undergo electronic excitation (63) was calculated for ternary complexes using the following equation.

$$E_{ads} = E_{nH2O/Ga-\alpha CD}^{tot} - E_{nH2O}^{tot} - E_{Ga-\alpha CD}^{tot}$$

Where $E_{nH2O/Ga-\alpha CD}^{tot}$ is the total energy of the adsorption system, $E_{nH2O}^{tot}$ is the total energy of the intact water molecules and $E_{Ga-\alpha CD}^{tot}$ is the energy of binary complex of Ga-αCD.
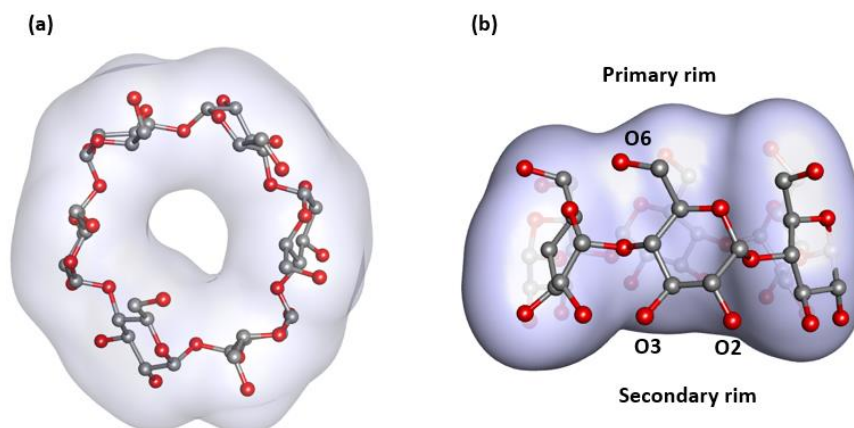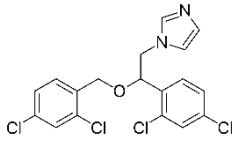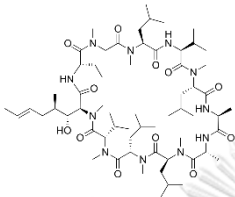
**Figure 16**. 3D structure of αCD (a) top view (b) side view representing primary and secondary rim.

3.2.5 Effect of guest molecules on the RCP and binding properties

To determine the drug binding capacity of neat αCD and ^{68}Ga-αCD, miconazole and cyclosporin A were selected as guest molecules because they favor αCD cavity and are representative of small and large molecular weight, respectively (64, 65). The chemical structures and physicochemical properties of miconazole and cyclosporin A are present in Table 3. Briefly, an excess amount of miconazole or cyclosporin A was added to αCD solution (1% w/v) to obtain drug saturation. The obtained drug suspension was agitated in an incubation shaker at $30 \pm 1$ °C, 150 rpm, for 24 h. After equilibrium is attained, 100 µl of each sample was pipetted and then mixed with 2 ml of 2% (w/v) sodium ascorbate solution. Finally, the sample was subjected to the radiolabeling process as previously described.

**Table   3.** Chemical structure and physicochemical properties of miconazole and cyclosporin A

| Drug | Chemical structure | Molecular weight (g/mol) | Log P | Solubility in water at 25 °C | Ref. |
|---|---|---|---|---|---|
| Miconazole | | 416.1 | 5.86 | 0.7 µg/ml | (66) |
| Cyclosporin A | | 1202.6 | 2.92 | 27 µg/ml | (67, 68) |

### 3.2.6 Statistical analysis

All quantitative data are presented as the mean ± standard deviation (SD). The statistical significance of the difference in mean was calculated by paired T test or one-way ANOVA followed by Post Hoc test. A $p < 0.01$ was considered as statistical significance.

จุฬาลงกรณ์มหาวิทยาลัย

CHULALONGKORN UNIVERSITY

# Chapter IV

# Results and Discussion

## 4.1 Identification and characterization of $^{68}$Ga-αCD

**4.**1.1 Mass spectrometry

As described earlier, Ga-68 completely decayed into Zn-68, and thus MS of $^{68}$Ga-αCD was determined in form of $^{68}$Zn-αCD. Since Zn-68 has a molecular weight of 68 and αCD has molecular weight of 972.3, the expected mass-to-charge ratio of $^{68}$Zn-αCD is 1041.3 Da, assuming that the final product ($^{68}$Zn-αCD) is 1:1 complex. The mass-to-charge of $^{68}$Zn-αCD in different ratios is shown in Table 4. Each m/z value is calculated by the following equation (69):

$$(m/z) = [M+zmH+]/z$$

Where M is monoisotopic mass, mH+ = proton mass and z is charge state.

ESI is an ionization technique in mass spectrometry. The electrostatic spray the injected solution in high electric field at the capillary tip, leading to the formation of a fine aerosol of charged droplets (70). Figure 17A shows the full ESI (+) triple quadrupole MS spectrum of the samples. A peak at 261.1 Da is observed which is aligned with the calculated m/z [1040.3+(4x1)]/4 = 261.08, representing a 1:1 complex of $^{68}$Zn-αCD (M+4H)$^{4+}$. No other complexations, e.g., 1:2 or 1:3 complex was found.

**Table 4.** Mass-to-charge of $^{68}$Zn-αCD in different ratios.

| Charge value | Mass-to-charge of $^{68}$Zn-αCD (Da) | | | | |
|---|---|---|---|---|---|
| | 1:1 | 2:1 | 3:1 | 1:2 | 1:3 |
| 1 | 1041.3 | 1109.3 | 1177.3 | 2013.6 | 2850.9 |
| 2 | 521.15 | 555.15 | 589.15 | 1007.3 | 1425.95 |
| 3 | 347.77 | 370.43 | 393.1 | 671.87 | 950.97 |
| 4 | 261.08 | 278.08 | 295.08 | 504.15 | 713.475 |
| 5 | 209.06 | 222.66 | 236.26 | 403.52 | 570.98 |
| 6 | 174.38 | 185.72 | 197.05 | 336.43 | 475.98 |
| 7 | 149.61 | 159.33 | 169.04 | 288.51 | 408.13 |
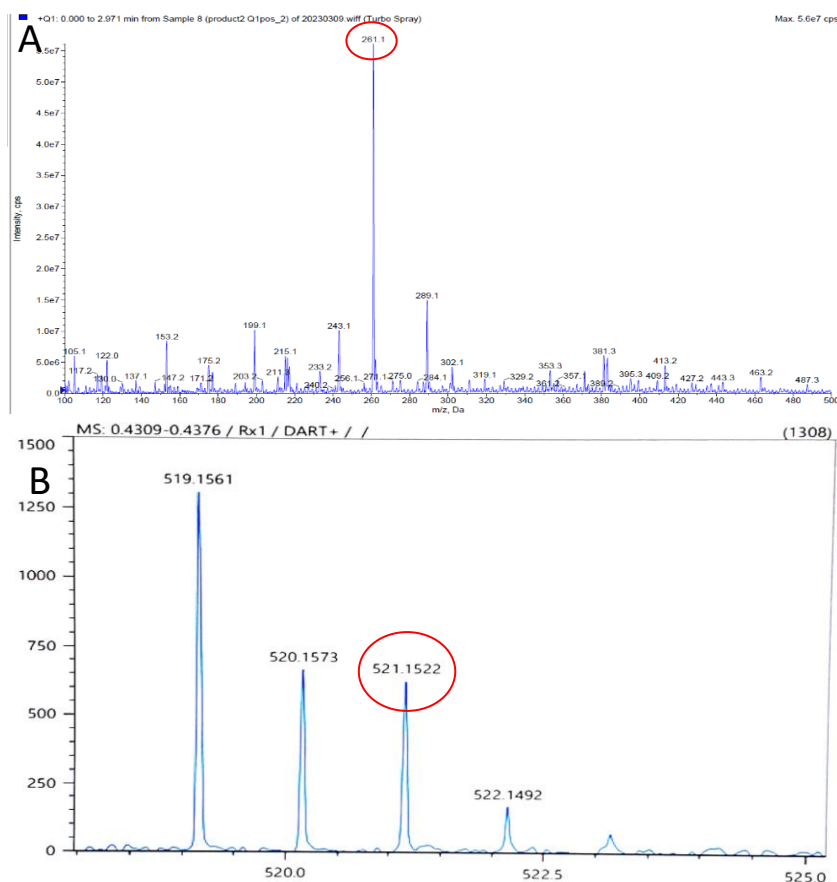
**Figure 17**. ESI (+) triple quadrupole MS spectrum (A) and DART (+) time of flight MS spectrum (B) of $^{68}$Zn-αCD

DART is another ionization technique in MS. It uses a stream of gas, like Helium, to interact with the sample. This interaction generates ions from the sample surface, which are then introduced into the mass spectrometer for analysis (71). Figure 17B shows DART (+) time of flight MS. The peak at 521.15 Da is observed, which is aligned with the calculated m/z [1040.3+(2x1)]/2 = 521.15 Da, representing a 1:1 complex of $^{68}$Zn-αCD $(M+2H)^{2+}$. The obtained results from both MS supported that $^{68}$Ga-αCD was formed with the stoichiometry ratio of 1:1 complex of $^{68}$Zn-αCD in the final solution.

**4.**1.2 *In silico* computational study

Theoretical methods, particularly spin-unrestricted density functional theory (UDFT) calculations, have played a crucial role in providing insights into the electronic structure of active species and plausible reaction mechanisms (72). We used CPCM as an implicit water model to evaluate the behavior of complexes in an aqueous environment. The result shows that $Ga^{3+}$ interacted with four explicit water molecules and two O6 at the primary rim and O2-O3 at the secondary rim of αCD, depicted in Figure 18, making a total of six coordination numbers which is in agreement with the reported study (73). There is a significant difference between the adsorption energies of $Ga^{3+}$ at the primary rim (- 81.57 kcal/mol) and secondary rim (-119.22 kcal/mol), which could be due to electrostatic interactions and hydrogen bonding in the implicit aqueous medium (74, 75). These findings are consistent with the MS data, indicating that Ga-68 has an affinity for αCD with a stoichiometry ratio of 1:1 in the complex.
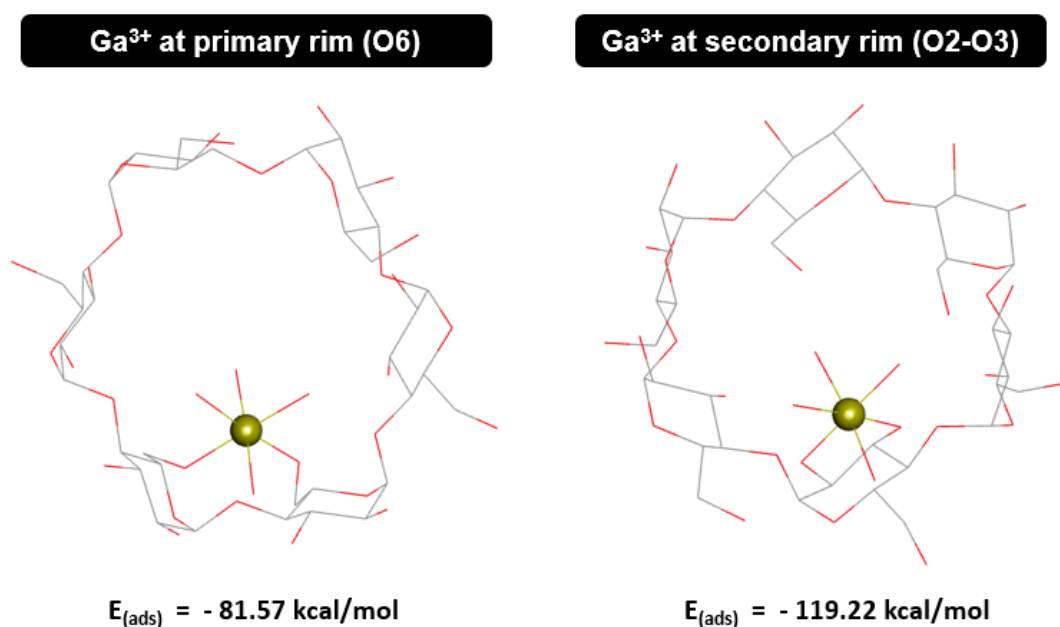


**Figure 18**. Top view of complexes with $Ga^{3+}$ cation.

The CD skeletons are depicted as wireframes, while the metal cations are represented as spheres, connected with four water molecules.

**4.2 Optimization of radiosynthesis of $^{68}$Ga-DOTA and $^{68}$Ga-αCD**

Table 5 displays the pH and the RCP of $^{68}$Ga-DOTA and $^{68}$Ga-αCD in the presence and absence of radiostabilizer. In the absence of radiostabilizer, the RCP of both samples are relatively low. As expected, the RCP of $^{68}$Ga-DOTA and $^{68}$Ga-αCD was 13.68% and 0.24%, respectively. According to diluted HCl as a solvent of both $^{68}$Ga-DOTA and $^{68}$Ga-αCD, the solutions were highly acidic with the pH of 1.55 and 1.56, respectively. To improve the RCP of these synthesized compounds, the addition of radiostabilizer was further investigated.

**Table 5.** pH and the radiochemical purity of $^{68}$Ga-DOTA and $^{68}$Ga-αCD

| Radiopharmaceuticals | Radiostabilizer | pH | Radiochemical purity (RCP, %) | RCP ratio[a] |
|---|---|---|---|---|
| $^{68}$Ga-DOTA | - | 1.55 ± 0.03 | 13.68 ± 0.69% | - |
| | Ascorbic acid | 2.02 ± 0.12 | 60.57 ± 5.68%[*] | 4.43 |
| | Sodium ascorbate | 3.83 ± 0.29 | 94.56 ± 1.34%[*] | 6.91 |
| $^{68}$Ga-αCD | - | 1.56 ± 0.02 | 0.24 ± 0.03% | - |
| | Ascorbic acid | 2.07 ± 0.23 | 0.59 ± 0.29% | 2.46 |
| | Sodium ascorbate | 3.93 ± 0.19 | 4.19 ± 0.25%[*] | 17.46 |

[a] ratio of RCP of the sample in presence of radiostabilizer/the absence of radiostabilizer. *Statistical difference (* $p < 0.01$) when compared to the absence of radiostabilizer

4.2.1 Effect of radiostabilizers

In both cases ($^{68}$Ga-DOTA and $^{68}$Ga-αCD), the RCP obtained from sodium ascorbate as a radiostabilizer yields significantly higher than those of ascorbic acid ($p < 0.01$), followed by those of without radiostabilizer. It indicates that radiostabilizer has a strongly positive effect on RCP in the radiolabeling process. A radiostabilizer also known as radioprotectant, is a radical scavenger that can prevent the formation of free radicals, which are induced by radiation emitted from radionuclide. These free radicals can degrade compounds or prevention formation of desired product (10, 49-51). Regarding to the pH of solutions, in the presence of ascorbic acid, the pH of

$^{68}$Ga-DOTA and $^{68}$Ga-αCD solutions were about 2.0, while that of sodium ascorbate were significantly higher (3.8–4.0) compared to the former cases ($p < 0.01$). Baudhuin et al. (50) investigated the effect of various radiostabilizers on $^{68}$Ga-NOTA-single-domain antibodies radiolabeling. Their result indicates ascorbic acid and gentisic acid are not well compatible with Ga-68. Based on our results, it clearly demonstrated that ascorbic acid was less potent than sodium ascorbate. This was assumed that the obtained RCP possibly be related to the pH of the sample. Optimal pH range for Ga-68 radiolabeling is ranging from 3 to 5 (76, 77). At pH lower than 3, the solution is too acidic for radiolabeling, whereas at pH above 5, $^{68}$GaCl$_3$ forms complex with hydroxide and become $^{68}$Ga(OH)$_3$, which is incapable of radiolabeling (76). Thus, in our case, the pH of the samples that comprise of sodium ascorbate are within the optimum range, which is suitable for Ga-68 radiolabeling, especially in case of $^{68}$Ga-DOTA exhibited the RCP value up to 95%. Our findings strengthen the strong binding affinity between DOTA and Ga-68. DOTA is a very well-known and commonly used bifunctional chelator for radiometal in nuclear medicine. Its cyclic structure offers an exceptional binding affinity with high thermodynamic stability. This ensures that once the radiometal is chelated inside, it remains securely bound without dissociated (78, 79). Interestingly, our synthesized $^{68}$Ga-αCD using sodium ascorbate as a potent radiostabilizer could generate 17.5 times higher than that using ascorbic acid. Sodium ascorbate, acting as an antioxidant, is biocompatible and also possesses a neutral and non-toxic substance. As the sodium salt of ascorbic acid, it is a water-soluble compound exhibiting potent antioxidant properties with low toxicity (80, 81). In order to confirm that sodium ascorbate does not compete with αCD or DOTA in radiosynthesis process, radiolabeling of $^{68}$GaCl$_3$ and sodium ascorbate (without ligand i.e, DOTA or αCD) was carried out. The result showed that the pH of final solution was about 2, which was not the optimal pH for radiolabeling and there was barely any activity on the product section of iTLC paper (RCP $\approx$ 0.01%). This indicates that sodium ascorbate did not interact with $^{68}$GaCl$_3$. Because $^{68}$Ga-DOTA and $^{68}$Ga-αCD using sodium ascorbate as a radiostabilizer showed a promising RCP result, their iTLC papers were further scanned by TLC scanner. Figure 19A and B display thin layer chromatograms of $^{68}$Ga-DOTA and $^{68}$Ga-αCD, respectively. The products namely $^{68}$Ga-DOTA and $^{68}$Ga-αCD were shown in red, while free Ga-68 was

shown in green. Retention factor (Rf) of $^{68}$Ga-DOTA and $^{68}$Ga-αCD were 0.77 and 0.72, respectively. The results from the scanner are aligned with the RCP, $^{68}$Ga-DOTA shows the product yield larger than free Ga-68. This is attributed to the strong preference of Ga$^{3+}$ ions for the DOTA cavity (79). In contrast, $^{68}$Ga-αCD exhibited a large amount of free Ga-68 together with low product yield. This is likely because the Ga-68 does not bind firmly to αCD like it does with the DOTA. This is supported by the result from *in silico* computational study which reveals that Ga-68 binds two OH groups of αCD and four water molecules. These observations support the result obtained by RCP measurement.
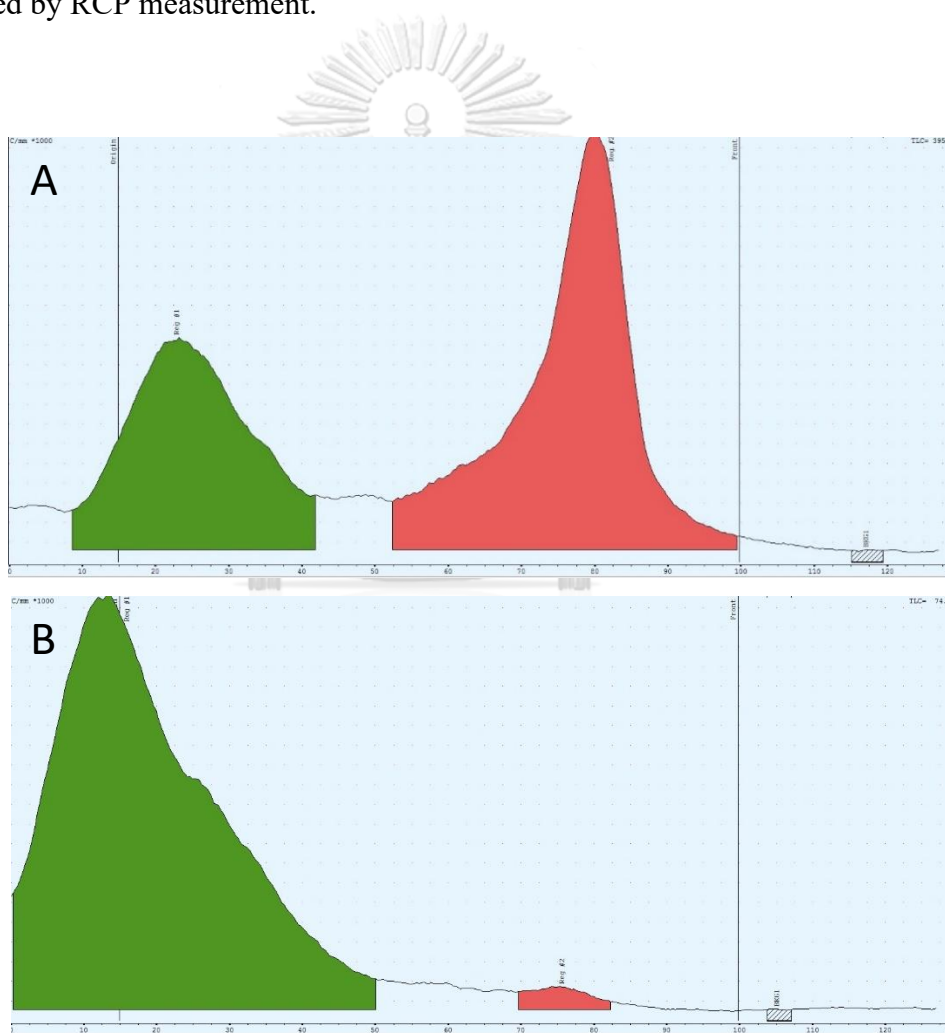


**Figure 19.** Thin layer chromatograms of $^{68}$Ga-DOTA (A) and $^{68}$Ga-αCD (B). The products that are 68Ga-DOTA and 68Ga-αCD are present in red (A and B, respectively), while free Ga-68 is present in green.

4.2.2 Effect of αCD concentrations and αCD polymer

The effect of αCD concentrations as a ligand on RCP of $^{68}$Ga-αCD was determined for the optimization parameter of radiosynthesis. The αCD concentration used in the study ranged from 2 to 20-folds compared to the initial step. Figure 16 displays the effect of αCD concentrations on the RCP of $^{68}$Ga-αCD. It divided into two parts where the RCP was increased with increasing αCD until its concentration of 1 mg/ml, which yielded the highest RCP (6.18 ± 0.16%) and then levelling off. This assumes that the saturation between Ga$^{3+}$ ion and ligand has been attained. αCD concentrations at 0.5 mg/ml and 1 mg/ml did not show a significant difference in RCP ($p > 0.01$). However, 1 mg/ml αCD was selected for further studies because it yielded the highest RCP. Comparison between each αCD concentration was shown in figure 20.
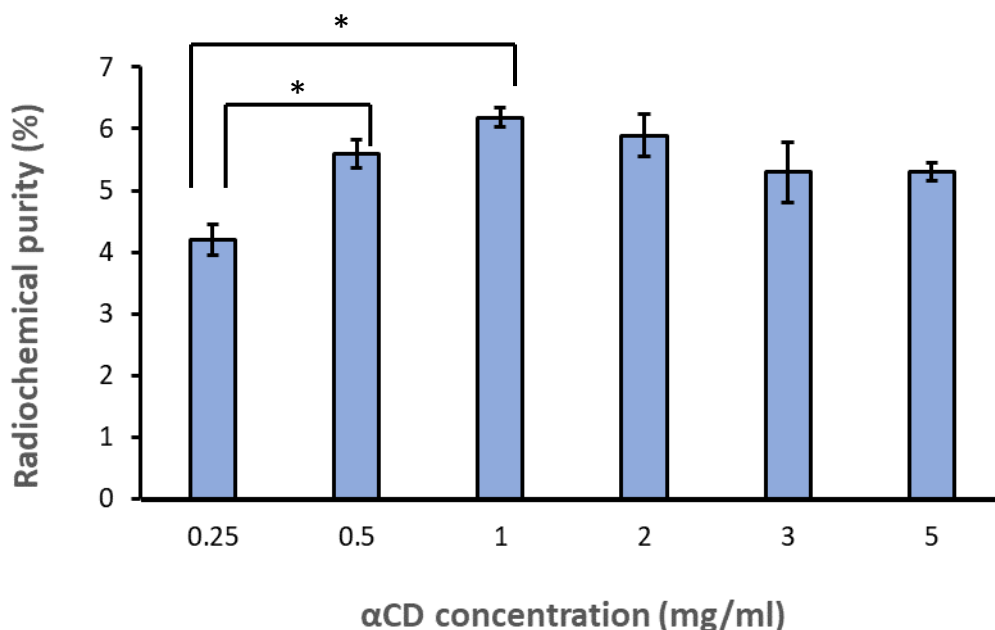


**Figure 20**. The effect of concentrations of αCD on the radiochemical purity of $^{68}$Ga-αCD. *Statistical difference (*p < 0.01) when compared to the initial αCD concentration (0.25 mg/ml).

To assess the impact of its three-dimensional configuration on labeling affinity with Ga-68, αCD polymer crosslinked with epichlorohydrin at the same concentration as αCD (1 mg/ml) was used. Epichlorohydrin is a widely used cross-linking agent. It forms the bond with CDs at the OH group on either primary or secondary rim. The polymerization of CDs with epichlorohydrin results in the creation of a 3D polymer network. This network offer an effective enhancement in drug delivery, contributing to the improved solubility and bioavailability of encapsulated drugs (82). The preliminary results reveal a pH value of $4.12 \pm 0.2$ and an obtained RCP of $5.49 \pm 0.57\%$. This resulting RCP is slightly lower than that achieved with the 1 mg/ml αCD solution ($6.18 \pm 0.16\%$). Although the CD polymer has additional binding sites derived from the polymer network, it appears that Ga-68 cannot bind within this polymer network. Instead, the substituent groups (i.e., epichlorohydrin) may hinder Ga-68 from binding to O6 at the primary rim and O2-O3 at the secondary rim of αCD. However, further studies are required to support this assumption. Nevertheless, given the lack of a significant difference in RCP between αCD and its polymer, αCD polymer was discarded for further studies.

## 4.2.3 Purification of $^{68}$Ga-αCD

It was found that the utilization of a C-18 cartridge for purification is a notable increase in the RCP. C-18 cartridge is a commonly used as a solid phase extraction cartridge for Ga-68 purification in clinical settings (10). C-18 cartridge comprises of octadecyl alkyl hydrocarbon chain (C18) which binds to the silica material and provides the column with hydrophobic properties, enabling the cartridge to trap non-polar or low polar compound inside the cartridge while allowing polar compound to pass through (83). Thus, the C-18 is able to trap our desired product ($^{68}$Ga-αCD) inside the column while free Ga-68 is discarded into waste vial. To get the desired product, C-18 will be eluted with solvents like ethanol and water (10). The final product after elution has a pH of $4.90 \pm 0.08$ which is higher than that form the unloaded C-18 cartridge that has pH value of $4.12 \pm 0.2$. Acidic pH likely due from hydrogen ions (H+) not being trapped inside the hydrophobic cartridge of C-18, allowing them to pass through and enter directly into the waste vial. This is consistent with the pH value of the waste vial which demonstrates a pH level of $4.12 \pm 0.06$,

closely resembling the condition without the loading of C-18. The final RCP of $^{68}$Ga-αCD is 18.42 ± 1.07%, which is a three-fold increase compared to no further purification step (6.18 ± 0.16%), (p<0.01). Despite the final RCP showing notable increases, it falls extremely below when compared to $^{68}$Ga-DOTA, which is able to achieve an impressive RCP of 94.56 ± 1.34% without any purification. The lower RCP observed in $^{68}$Ga-αCD may be attributed to the presence of some free Ga-68 within the product vial, potentially resulting from a high influx of free Ga-68, an incomplete separation between free Ga-68 and $^{68}$Ga-αCD, or the dissociation of some $^{68}$Ga-αCD back into free Ga-68.

According to the studies by Fuscaldi et al (57) the automatic synthesis module was employed to synthesize $^{68}$Ga-PSMA-11. Using the similar protocol of our study, they are able to achieve a remarkably high RCP at 95.59% with the use of a C-18 cartridge. This indicates that despite the C-18 cartridge having been proven itself several times in numerous clinical settings, it might not be the most optimal choice for $^{68}$Ga-αCD purification. According to the literature Ga-68 radiopharmaceutical RCP should exceed 90% in order to be applied in clinical setting (10, 57). Therefore, consideration of additional purification steps or exploring new techniques are required to achieve a higher RCP of $^{68}$Ga-αCD.

One of the potential approaches involves the utilization of size exclusion chromatography, which is also known as gel filtration chromatography. It is a commonly used technique to purify and separate different compounds based on their size distinction (84). In size exclusion chromatography, a porous material serves as the stationary phase. Small molecular compounds will fit within porous pore of stationary phase while large molecular compounds do not enter the pores and eluted through the column more rapidly (84). Consequently, molecules separate based on their size as they pass through the column and are eluted in order to decrease MW. The implementation of the size exclusion chromatography as a purification column could potentially help increase RCP of $^{68}$Ga-αCD. Its ability to retain small molecular compounds allows for the capture of unreacted free Ga-68 inside the column, while larger $^{68}$Ga-αCD passes through the column. Employing the size exclusion chromatography as a preliminary step before employing C-18 cartridge could

potentially alleviate the influx of free Ga-68 into subsequent purification step. Alternatively, it can be employed as a stand-alone method, letting it capture unreacted free Ga-68 and allowing the collection of pass-through fractions containing purified $^{68}$Ga-αCD.

Another potential approach is the utilization of ion exchange chromatography, a technique specifically designed for purification and separation of charge compounds from different charge or non-charge compounds. It principle is based on electrostatic interaction between the compound and the stationary phase (85). There are mainly two types of ion exchange chromatography which are cation and anion exchange chromatography. The cation exchange chromatography is comprised of negatively charged stationary phase which interact and retain positively charged compound in the interested product. On the other hand, the anion exchange chromatography featuring positively charge stationary phase which interact and retain negatively charged compound (85). Employing the cation exchange chromatography could potentially help increase RCP of $^{68}$Ga-αCD. Its ability to retain positive charge compound can be used to trap unreacted free Ga-68, while $^{68}$Ga-αCD is freely transverse through the column.

Employing the size exclusion or cation exchange chromatography as a preliminary step before employing C-18 cartridge could potentially alleviate the influx of free Ga-68 into subsequent purification step. Alternatively, either size exclusion or cation exchange chromatography can be employed as a stand-alone method, allowing the column to effectively capture unreacted free Ga-68, facilitating the collection of a fraction that contains purified $^{68}$Ga-αCD.

## 4.3 Effect of guest molecules on the RCP of $^{68}$Ga-αCD

According to the literature, Jóhannsdóttir and co-workers investigated the phase-solubility profiles of cyclosporin A and various CD types. It was found that αCD has greater solubilizing effect on cyclosporin A and provides higher complexing efficacy than the other CD tested (65). Fukuya et. Al (86) investigated the solubility and therapeutic effect of cyclosporin A/CD complex in inhalation dosage form for

asthma therapy. It was found that maltosyl-αCD (G2-αCD) was the most optimal choice for cyclosporin A/CD complex in inhalation dosage form. This CD inclusion complex provides solubilization enhancement, shows cilio-inhibition activity with low cytotoxicity. These observations demonstrate that cyclosporin A has higher affinity to CDs with relatively small cavities, forming water-soluble cyclosporin A/αCD complexes than larger CD cavities. In the case of miconazole/CD complexes, Tenjarla and co-worker investigated the CD solubilizing effect of miconazole for oral and topical delivery. The complex was prepared by lyophilization method. It was found that αCD significantly enhanced the aqueous solubility of miconazole compared to the larger CD cavities and their hydroxypropyl derivatives (i.e., βCD, γCD, HPβCD and HPγCD) (64). Murata et. al (87) investigated the solubility effect of various CDs on miconazole for oral Candidiasis treatment. It was found that αCD has a great solubilizer for miconazole, resulting in a 1.5-fold increase in its solubility. This demonstrates that miconazole also has higher affinity to CDs with relatively small cavities like αCD. Thus, cyclosporin A and miconazole were selected as model drugs due to that they have affinity to αCD cavity, and they can be used for parenteral preparations. Regards to molecular weight of cyclosporin A is 1202.6 Da (88) and that of miconazole is 416.13 Da (89), representing large and small molecule, respectively, the effect of these drugs on the RCP of $^{68}$Ga-αCD was further determined.

Table 6 shows pH and the RCP of $^{68}$Ga-miconazole-αCD and $^{68}$Ga-cyclosporin A-αCD complexes. The radiolabeling of miconazole-αCD and cyclosporin A-αCD complexes results in RCP that insignificantly difference compared to the neat $^{68}$Ga-αCD. $^{68}$Ga-miconazole-αCD complex demonstrates an RCP of 18.68 ± 1.69%, whereas $^{68}$Ga-cyclosporin A-αCD complex exhibits an RCP of 19.19 ± 1.35%. For the pH of solutions, it also has shown that with and without drugs, the pH was not altered. These findings indicate that the encapsulation of drugs within αCD cavity does not interfere with the Ga$^{3+}$ ion binding affinity.

*In silico* computational data as shown in Figure 18 support the effect of miconazole and cyclosporin A on binding affinity between Ga-68 and αCD. Given that Ga-68 can bind to the either primary or secondary rim of αCD, while either

miconazole or cyclosporin A bind inside the αCD cavity. The RCP of ^{68}Ga-miconazole-αCD and ^{68}Ga-cyclosporin A-αCD are aligned with drug free ^{68}Ga-αCD. Overall, the proposed ^{68}Ga-miconazole-αCD and ^{68}Ga-cyclosporin A-αCD configurations are shown in Figure 21. Additionally, this finding emphasizes the significant potential of ^{68}Ga-αCD for further exploration, assuming that small or large drug molecules can be used to co-deliver with ^{68}Ga-αCD. This presents a valuable avenue for gaining insight into the biodistribution and pharmacokinetic data of the specific drug. Moreover, our findings also pioneered present the possibility for therapeutic application, especially in cancer treatment. It is suggested that substituting Ga-68 with Lu-177 and employed alongside cancer drug might offer a synergistic effect on treatment of cancer.

**Table 6.** pH and the radiochemical purity of ^{68}Ga-miconazole-αCD and ^{68}Ga-cyclosporin A-αCD complexes

| Radiopharmaceuticals | pH | Radiochemical purity (RCP, %) | RCP ratio[a] |
|---|---|---|---|
| ^{68}Ga-αCD | $4.90 \pm 0.08$ | $18.42 \pm 1.07\%$ | - |
| ^{68}Ga-miconazole-αCD | $4.96 \pm 0.23$ | $18.68 \pm 1.69\%$ | 1.01 |
| ^{68}Ga-cyclosporin A-αCD | $4.97 \pm 0.08$ | $19.19 \pm 1.35\%$ | 1.04 |

[a] ratio of RCP of the sample in presence of drug molecule/the absence of drug molecule
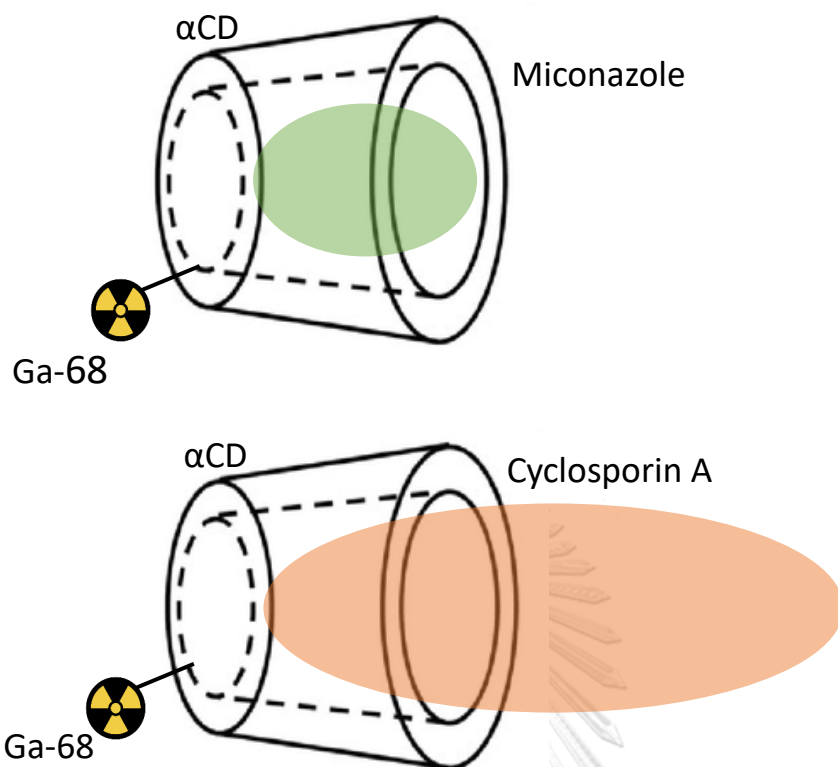
**Figure 21.** Proposed configuration of ^{68}Ga-miconazole-αCD and ^{68}Ga-cyclosporin A-αCD

# Chapter V
# Conclusion

CDs are commonly used as pharmaceutical excipients, which well-known for their ability to form inclusion complexes with poorly water-soluble drugs. They offer versatile benefits in many industries, such as food, textiles and packaging, cosmetics and personal care, etc. Recently, CDs have been promising for the application of medical imaging, particularly in the development and formulation of radiopharmaceuticals for nuclear medicine imaging. In this study, we focus exclusively on the complex formation of Ga-68 and αCD. To the best of our knowledge, we believed we were pioneering to achieve the successful radiosynthesis of $^{68}$Ga-αCD without an additional chelator molecule by direct radiolabeling of Ga-68 with αCD. The results obtained from the MS demonstrated that $^{68}$Ga-αCD was formed with the stoichiometry ratio of 1:1 complex of $^{68}$Zn-αCD. This ratio is also confirmed by an *in silico* computational study, which also determined the binding site of Ga-68 at either the primary or secondary rim of αCD. Initially, the RCP of $^{68}$Ga-αCD is very low. The RCP is increased when using the appropriate radiostabilizer and optimized process. In our present study, it suggested that using sodium ascorbate as a radiostabilizer, the concentration of 1 mg/ml αCD and the C-18 cartridge for purification were the optimal parameters for radiolabeling $^{68}$Ga-αCD. Incorporating drugs either miconazole or cyclosporin A in αCD solutions, forming drug/αCD inclusion complex before subjected to radiolabeling, did not interfere the binding affinity between Ga-68 and αCD. Consequently, $^{68}$Ga-αCD can be used for drug-load for radiopharmaceutical applications. Our findings present the simply radiosynthesis process and obtain the promising novel synthesized $^{68}$Ga-αCD used in the field of medical imaging. However, our novel radiopharmaceutical is currently not ready for clinical use. It was noted that further improving the optimization of synthesized $^{68}$Ga-αCD is required to obtain the higher RCP of $^{68}$Ga-αCD together with lower free Ga-68. These enhancements are essential for the appropriate utilization of this novel radiopharmaceuticals in a clinical setting. Additionally, larger CDs i.e., βCD, γCD as ligands are also interested in CD-based Ga-68 radiosynthesis.

# REFERENCES

1. Jansook P, Ogawa N, Loftsson T. Cyclodextrins: structure, physicochemical properties and pharmaceutical applications. Int J Pharm. 2018;535(1-2):272-84.

2. Jansook P, Hnin HM, Loftsson T, Stefansson E. Cyclodextrin-based formulation of carbonic anhydrase inhibitors for ocular delivery - A review. Int J Pharm. 2021;606:120955.

3. Shepelytskyi Y, Newman CJ, Grynko V, Seveney LE, DeBoef B, Hane FT, et al. Cyclodextrin-based contrast agents for medical imaging. Molecules. 2020;25(23).

4. Sureshkumar A, Hansen B, Ersahin D. Role of nuclear medicine in imaging. Semin Ultrasound CT MR. 2020;41(1):10-9.

5. Ge J, Zhang Q, Zeng J, Gu Z, Gao M. Radiolabeling nanomaterials for multimodality imaging: New insights into nuclear medicine and cancer diagnosis. Biomaterials. 2020;228:119553.

6. Morris ZS, Wang AZ, Knox SJ. The radiobiology of radiopharmaceuticals. Semin Radiat Oncol. 2021;31(1):20-7.

7. Kunos CA, Mankoff DA, Schultz MK, Graves SA, Pryma DA. Radiopharmaceutical chemistry and drug development-what's changed? Semin Radiat Oncol. 2021;31(1):3-11.

8. Sunderland JJ, Ponto LB, Capala J. Radiopharmaceutical delivery for theranostics: pharmacokinetics and pharmacodynamics. Semin Radiat Oncol. 2021;31(1):12-9.

9. Konik A, O'Donoghue JA, Wahl RL, Graham MM, Van den Abbeele AD. Theranostics: The role of quantitative nuclear medicine imaging. Semin Radiat Oncol. 2021;31(1):28-36.

10. Nelson BJB, Andersson JD, Wuest F, Spreckelmeyer S. Good practices for (68)Ga radiopharmaceutical production. EJNMMI Radiopharm Chem. 2022;7(1):27.

11. Hajdu I, Angyal J, Szikra D, Kertesz I, Malanga M, Fenyvesi E, et al. Radiochemical synthesis and preclinical evaluation of (68)Ga-labeled NODAGA-hydroxypropyl-beta-cyclodextrin ((68)Ga-NODAGA-HPBCD). Eur J Pharm Sci. 2019;128:202-8.

12. Trencsenyi G, Kis A, Szabo JP, Rati A, Csige K, Fenyvesi E, et al. In vivo

preclinical evaluation of the new (68)Ga-labeled beta-cyclodextrin in prostaglandin E2 (PGE2) positive tumor model using positron emission tomography. Int J Pharm. 2020;576:118954.

13.     Csige K, Szabo JP, Kalman-Szabo I, Denes NS, Szikra D, Kepes Z, et al. In vivo investigation of Gallium-68 and Bismuth-205/206 labeled beta cyclodextrin for targeted alpha therapy of prostaglandin E2 receptor-expressing tumors in mice. Int J Pharm. 2022;625:122132.

14.     Szabo JP, Csige K, Kalman-Szabo I, Arato V, Opposits G, Joszai I, et al. In vivo assessment of tumor targeting potential of (68)Ga-labelled randomly methylated beta-cyclodextrin (RAMEB) and 2-hydroxypropyl-beta-cyclodextrin (HPbetaCD) using positron emission tomography. Int J Pharm. 2022;630:122462.

15.     Lorenzo-Veiga B, Alvarez-Lorenzo C, Loftsson T, Sigurdsson HH. Age-related ocular conditions: Current treatments and role of cyclodextrin-based nanotherapies. Int J Pharm. 2021;603:120707.

16.     Soe H, Maw PD, Loftsson T, Jansook P. A current overview of cyclodextrin-based nanocarriers for enhanced antifungal delivery. Pharmaceuticals (Basel). 2022;15(12).

17.     Lai W-F. Chapter 5 - Design of cyclodextrin-based systems for intervention execution. In: Lai W-F, editor. Delivery of Therapeutics for Biogerontological Interventions: Academic Press; 2019. p. 49-59.

18.     Khan AR FP, Stine KJ, D'Ssouza VT. Methods for selective modifications of cyclodextrins. Chem Rev. 1997;98:1977-96.

19.     Przybyla MA, Yilmaz G, Becer CR. Natural cyclodextrins and their derivatives for polymer synthesis. Polymer Chemistry. 2020;11(48):7582-602.

20.     Vermeulen K, Vandamme M, Bormans G, Cleeren F. Design and challenges of radiopharmaceuticals. Semin Nucl Med. 2019;49(5):339-56.

21.     English KK, Knox S, Graves SA, Kiess AP. Basics of physics and radiobiology for radiopharmaceutical therapies. Pract Radiat Oncol. 2022;12(4):289-93.

22.     Shende P, Gandhi S. Current strategies of radiopharmaceuticals in theranostic applications. Journal of Drug Delivery Science and Technology. 2021;64.

23.     Kiraga Ł, Kucharzewska P, Paisey S, Cheda Ł, Domańska A, Rogulski Z, et al.

Nuclear imaging for immune cell tracking in vivo – Comparison of various cell labeling methods and their application. Coord Chem Rev. 2021;445.

24.     Vallabhajosula S, Solnes L, Vallabhajosula B. A broad overview of positron emission tomography radiopharmaceuticals and clinical applications: what is new? Semin Nucl Med. 2011;41(4):246-64.

25.     Kawada K, Iwamoto M, Sakai Y. Mechanisms underlying (18)F-fluorodeoxyglucose accumulation in colorectal cancer. World J Radiol. 2016;8(11):880-6.

26.     Ziessman HA, O'Malley JP, Thrall JH. Skeletal scintigraphy.  Nuclear Medicine2014. p. 98-130.

27.     Alqahtani FF. SPECT/CT and PET/CT, related radiopharmaceuticals, and areas of application and comparison. Saudi Pharm J. 2023;31(2):312-28.

28.     Hashimoto H, Nakanishi R, Mizumura S, Hashimoto Y, Okamura Y, Yamanaka K, et al. Prognostic value of (99m)Tc-ECD brain perfusion SPECT in patients with atrial fibrillation and dementia. EJNMMI Res. 2020;10(1):3.

29.     Kim S, Mountz JM. SPECT imaging of Epilepsy: An overview and comparison with F-18 FDG PET. Int J Mol Imaging. 2011;2011:813028.

30.     ITOH K. Review of pharmacokinetics, clinical application to renal diseases and quantification of renal function. Annals of Nuclear Medicine. 2001;15(3):179-90.

31.     Busk M, Sinning S, Alstrup AKO, Munk OL, Vendelbo MH. Nuclear medicine preclinical research: the role of cell cultures. Semin Nucl Med. 2023;53(5):558-69.

32.     Kim MH, Lee YJ, Kang JH. Stem cell monitoring with a direct or indirect labeling method. Nucl Med Mol Imaging. 2016;50(4):275-83.

33.     Krekorian M, Fruhwirth GO, Srinivas M, Figdor CG, Heskamp S, Witney TH, et al. Imaging of T-cells and their responses during anti-cancer immunotherapy. Theranostics. 2019;9(25):7924-47.

34.     Sriprapa T, Doungta T, Sakulsamart N, Taweewatthanasopon N, Madputeh L, Ragchana P, et al. Evaluation of the sfficacy and safety of the ITM 68Ge/68Ga generator after its recommended shelf-life. SMJ. 2023;75(10):752-8.

35.     Gillings N. Quality control of radiopharmaceuticals: Basics and instrumentation. Nuclear Medicine and Molecular Imaging2022. p. 250-9.

36.     Vallabhajosula S, Killeen RP, Osborne JR. Altered biodistribution of radiopharmaceuticals: role of radiochemical/pharmaceutical purity, physiological, and pharmacologic factors. Semin Nucl Med. 2010;40(4):220-41.

37.     Liu F, Yoho M, Tsai H, Fernando K, Tisdale J, Shrestha S, et al. The working principle of hybrid perovskite gamma-ray photon counter. Mater Today. 2020;37:27-34.

38.     Gillings N, Hjelstuen O, Ballinger J, Behe M, Decristoforo C, Elsinga P, et al. Guideline on current good radiopharmacy practice (cGRPP) for the small-scale preparation of radiopharmaceuticals. EJNMMI Radiopharm Chem. 2021;6(1):8.

39.     Aungurarat A, Ngamprayad U. Chemical and biological control of MDP complex. Bangkok: Office of Atomic Energy of Peace, Ministry of Science, Technology and Environment; 1993 1993 Jul.  Contract No.: ISBN9747400499.

40.     Romero E, Martinez A, Oteo M, Ibanez M, Santos M, Morcillo MA. Development and long-term evaluation of a new (68)Ge/(68)Ga generator based on nano-SnO(2) for PET imaging. Sci Rep. 2020;10(1):12756.

41.     Evans HL, Carroll L, Aboagye EO, Spivey AC. Bioorthogonal chemistry for (68) Ga radiolabelling of DOTA-containing compounds. J Labelled Comp Radiopharm. 2014;57(4):291-7.

42.     Zhou X, Dong L-L, Li Y, Cui M-C, Shen L-T. Design and synthesis of a new conjugate of a tris(3-hydroxy-4-pyridinone) chelator (KC18) for potential use as gallium-68-labeled prostate-specific membrane antigen (PSMA) radiopharmaceutical. Results in Chemistry. 2021;3.

43.     Onal C, Ozyigit G, Guler OC, Hurmuz P, Torun N, Tuncel M, et al. Role of 68-Ga-PSMA-PET/CT in pelvic radiotherapy field definitions for lymph node coverage in prostate cancer patients. Radiother Oncol. 2020;151:222-7.

44.     Kilian K. (68)Ga-DOTA and analogs: Current status and future perspectives. Rep Pract Oncol Radiother. 2014;19(Suppl):S13-S21.

45.     Cessna JT, Fitzgerald R, Zimmerman BE, Laureano-Perez L, Bergeron DE, van Wyngaardt F, et al. Results of an international comparison of activity measurements of (68)Ge. Appl Radiat Isot. 2018;134:385-90.

46.     Rosch F. Past, present and future of 68Ge/68Ga generators. Appl Radiat Isot. 2013;76:24-30.

47.    Velikyan I. 68Ga-based radiopharmaceuticals: production and application relationship. Molecules. 2015;20(7):12913-43.

48.    Michael M, Yury S, Elisabeth E. Gallium-68: Radiolabeling of Radiopharmaceuticals for PET Imaging - A Lot to Consider. In: Syed Ali Raza N, Muhammad Babar I, editors. Medical Isotopes. Rijeka: IntechOpen; 2019. p. Ch. 2.

49.    Chen J, Linder KE, Cagnolini A, Metcalfe E, Raju N, Tweedle MF, et al. Synthesis, stabilization and formulation of [177Lu]Lu-AMBA, a systemic radiotherapeutic agent for Gastrin Releasing Peptide receptor positive tumors. Appl Radiat Isot. 2008;66(4):497-505.

50.    Baudhuin H, Cousaert J, Vanwolleghem P, Raes G, Caveliers V, Keyaerts M, et al. (68)Ga-labeling: laying the foundation for an anti-radiolytic formulation for NOTA-sdAb PET tracers. Pharmaceuticals (Basel). 2021;14(5).

51.    Shuang Liu CEE, D. Scott Edwards. Ascorbic acid useful as a buffer agent and radiolytic stabilizer for metalloradiopharmaceuticals.pdf. Bioconjug Chem. 2003;14(5):1052-6.

52.    Bendich A, Machlin LJ, Scandurra O, Burton GW, Wayner DDM. The antioxidant role of vitamin C. Advances in Free Radical Biology & Medicine. 1986;2(2):419-44.

53.    Law G-L, Wong W-T. An introduction to molecular imaging. In: Long N, Wong W-T, editors. The Chemistry of Molecular Imaging. 1 ed: John Wiley & Sons, Inc; 2015.

54.    Shidahara M, Funaki Y, Watabe H. Noninvasive estimation of human radiation dosimetry of (18)F-FDG by whole-body small animal PET imaging in rats. Appl Radiat Isot. 2022;181:110071.

55.    Hu K, Wu W, Xie L, Geng H, Zhang Y, Hanyu M, et al. Whole-body PET tracking of a d-dodecapeptide and its radiotheranostic potential for PD-L1 overexpressing tumors. Acta Pharmaceutica Sinica B. 2021.

56.    Tsai YJ, Liu C. Pitfalls on PET/CT due to artifacts and instrumentation. Semin Nucl Med. 2021;51(6):646-56.

57.    Fuscaldi LL, Sobral DV, Durante ACR, Mendonca FF, Miranda ACC, da Cunha ML, et al. Standardization of the [(68)Ga]Ga-PSMA-11 radiolabeling protocol in an

automatic synthesis module: assessments for PET imaging of prostate cancer. Pharmaceuticals (Basel). 2021;14(5).

58.     Ferreira L, Campos J, Veiga F, Cardoso C, Paiva-Santos AC. Cyclodextrin-based delivery systems in parenteral formulations: A critical update review. Eur J Pharm Biopharm. 2022;178:35-52.

59.     Lepareur N. Cold kit labeling: The future of (68)Ga radiopharmaceuticals? Front Med (Lausanne). 2022;9:812050.

60.     Castner JF, Zdankiewicz DD, Anderson JE, inventors; ; Lantheus Medical Imaging Inc, assignee. Stabilization of radiopharmaceutical compositions using ascorbic acid patent US9687571B2. 2017 27 June.

61.     Stephens PJ, Devlin FJ, Chabalowski CF, Frisch MJ. Ab initio calculation of vibrational absorption and circular dichroism spectra using density functional force fields. J Phys Chem B. 1994;45.

62.     Barone V, Cossi M, Tomasi J. Geometry optimization of molecular structures in solution by the polarizable continuum model. J Comput Chem. 1998;19(4):404-17.

63.     Buemi G, Sergio Cataliotti R. The polarizable continuum potential model in the liquid state calculations. density functional computational analysis of the anharmonic vibrational spectrum of liquid water. J Mol Liq. 2021;340.

64.     Tenjarla S, Puranajoti P, Kasina R, Mandal T. Preparation, characterization, and evaluation of miconazole-cyclodextrin complexes for improved oral and topical delivery. J Pharm Sci. 1998;87(4):425-9.

65.     Johannsdottir S, Jansook P, Stefansson E, Loftsson T. Development of a cyclodextrin-based aqueous cyclosporin A eye drop formulations. Int J Pharm. 2015;493(1-2):86-95.

66.     Kelemen H, Hancu G, Gâz-Florea SA, Nemes-Nagy E, Papp LA, Mircia E. Characterization of inclusion complexes between miconazole and different cyclodextrin derivatives. Acta Medica Marisiensis. 2018;64(2):70-6.

67.     Wiącek AE, Jurak M, Ładniak A, Przykaza K, Szafran K. Cyclosporine CsA—the physicochemical characterization of liposomal and colloidal systems. Colloids and Interfaces. 2020;4(4).

68.     Guada M, Beloqui A, Kumar MN, Preat V, Dios-Vieitez Mdel C, Blanco-Prieto

MJ. Reformulating cyclosporine A (CsA): More than just a life cycle management strategy. J Control Release. 2016;225:269-82.

69.    Liepold L, Oltrogge LM, Suci PA, Young MJ, Douglas T. Correct charge state assignment of native electrospray spectra of protein complexes. J Am Soc Mass Spectrom. 2009;20(3):435-42.

70.    Glish GL, Vachet RW. The basics of mass spectrometry in the twenty-first century. Nat Rev Drug Discov. 2003;2(2):140-50.

71.    Osorio J, Aznar M, Nerin C, Elliott C, Chevallier O. Comparison of LC-ESI, DART, and ASAP for the analysis of oligomers migration from biopolymer food packaging materials in food (simulants). Anal Bioanal Chem. 2022;414(3):1335-45.

72.    Siegbahn PE. The performance of hybrid DFT for mechanisms involving transition metal complexes in enzymes. J Biol Inorg Chem. 2006;11(6):695-701.

73.    Wong TJWEH, Anderson GRWCJ. Coordinating radiometals of Copper, Gallium, Indium, Yttrium and Zirconium for PET and SPECT Imaging of disease. Chem Rev. 2010;5.

74.    Rezaeisadat M, Salehi N, Bordbar AK. Inclusion of Levodopa into beta-Cyclodextrin: A Comprehensive Computational Study. ACS Omega. 2021;6(37):23814-25.

75.    Stachowicz A, Styrcz A, Korchowiec J, Modaressi A, Rogalski M. DFT studies of cation binding by β-cyclodextrin. Theor Chem Acc. 2011;130(4-6):939-53.

76.    Suthiram J, Ebenhan T, Marjanovic-Painter B, Sathekge MM, Zeevaart JR. Towards facile radiolabeling and preparation of Gallium-68-/Bismuth-213-DOTA-[Thi(8), Met(O(2))(11)]-substance P for future clinical application: first experiences. Pharmaceutics. 2021;13(9).

77.    Bauwens M, Chekol R, Vanbilloen H, Bormans G, Verbruggen A. Optimal buffer choice of the radiosynthesis of (68)Ga-Dotatoc for clinical application. Nucl Med Commun. 2010;31(8):753-8.

78.    Baranyai Z, Tircsó G, Rösch F. The use of the macrocyclic chelator DOTA in radiochemical separations. Eur J Inorg Chem. 2019;2020(1):36-56.

79.    Liu X, Chen L, Li Y, He C, Zhang X, Zhou H, et al. Synthesis of novel DOTA-/AAZTA-based bifunctional chelators: Solution thermodynamics, peptidomimetic

conjugation, and radiopharmaceutical evaluation. Biomed Pharmacother. 2023;165:115114.

80. Virdah Dwi Dewantari, Setyabudi, Ismiyatin. K. Antioxidant potential of epigallocatechin-3-gallate, ascorbic acid, and sodium ascorbate. J Conserv Dent 2021;11.

81. Vidhya S, Srinivasulu S, Sujatha M, Mahalaxmi S. Effect of grape seed extract on the bond strength of bleached enamel. Oper Dent. 2011;36(4):433-8.

82. Gidwani B, Vyas A. Synthesis, characterization and application of epichlorohydrin-beta-cyclodextrin polymer. Colloids Surf B Biointerfaces. 2014;114:130-7.

83. Badawy MEI, El-Nouby MAM, Kimani PK, Lim LW, Rabea EI. A review of the modern principles and applications of solid-phase extraction techniques in chromatographic analysis. Anal Sci. 2022;38(12):1457-87.

84. Deb PK, Kokaz SF, Abed SN, Paradkar A, Tekade RK. Pharmaceutical and biomedical applications of polymers. Basic Fundamentals of Drug Delivery2019. p. 203-67.

85. Cummins PM, Rochfort, K.D., O'Connor, B.F. . Ion-exchange chromatography. In: Walls D, Loughran S, editors. Protein Chromatography Methods in Molecular Biology. 1485. New York: Humana Press; 2017.

86. Fukaya H, Iimura A, Hoshiko K, Fuyumuro T, Noji S, Nabeshima T. A cyclosporin A/maltosyl-alpha-cyclodextrin complex for inhalation therapy of asthma. Eur Respir J. 2003;22(2):213-9.

87. Murata Y, Kofuji K, Nakano S, Kamaguchi R. Cyclodextrin-modified film dosage forms for oral candidiasis treatment. Pharmacology &amp; Pharmacy. 2015;06(05):247-53.

88. Survase SA, Kagliwal LD, Annapure US, Singhal RS. Cyclosporin A--a review on fermentative production, downstream processing and pharmacological applications. Biotechnol Adv. 2011;29(4):418-35.

89. Al-Badr AA. Miconazole nitrate: comprehensive profile. Profiles Drug Subst Excip Relat Methodol. 2005;32:3-65.

# VITA

| | |
|---|---|
| **NAME** | Sirapop Sriaumpai |
| **DATE OF BIRTH** | 9 October 1997 |
| **PLACE OF BIRTH** | Bangkok, Thailand |
| **INSTITUTIONS ATTENDED** | Chulalongkorn university |
| **HOME ADDRESS** | 157, soi 22, chaloem phra kiat rama 9 road, Nong Bon sub-district, Prawet district, Bangkok, Thailand, 10250. |
| **AWARD RECEIVED** | Outstanding Poster Presentation in The 23rd International Conference of Public Health Sciences "Sustainable Public Health : Innovations for Global Impact" |